ON-LINE PROTECTION OF POWER TRANSFORMER USING MICROPROCESSOR

A Thesis Submitted
In Partial Fulfilment of the Requirements
for the Degree of

MASTER OF TECHNOLOGY

by
ARUN SINGHAL

to the

DEPARTMENT OF ELECTRICAL ENGINEERING

INDIAN INSTITUTE OF TECHNOLOGY, KANPUR

MAY, 1987

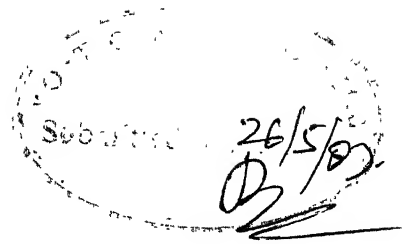

CERTIFICATE

Certified that the work entitled 'On-line protection of power transformer using microprocessor' which is being submitted by Mr. Arun Singhal in partial fulfilment of the award of the degree of Master of Technology, has been carried out under my supervision and guidance. The matter presented in this thesis dissertation has not been submitted elsewhere for a degree.

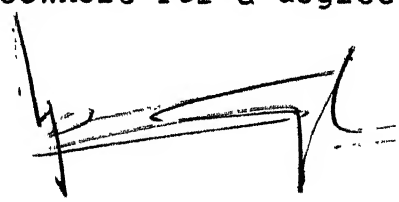

Dr. L.P. Singh
Professor
E. E. Dept.
I.I.T. Kanpur

ACKNOWLEDGEMENTS

I wish to express my heartiest gratitude to Dr. L.P. Singh, who has been guiding me, not only during the formulation of the present work, but throughout my long stay at IIT Kanpur. This work has become a reality only because of his extremely understanding attitude and unwavering support.

My thanks are also due to Mr. B. Nandy, Mr. G.N.M. Sudhakar and Mr. Prem Mehrotra for the help they provided towards the development and testing of the hardware, as well as simulation of the relay performance.

I shall always remain indebted to Dr. K.R. Srivathsan, who is to be given credit for a substantial amount of the knowledge gained by me as an engineer.

No words of thanks are sufficient to express my gratitude to my friends and colleagues, Mr. V.P. Singh and Mr. Arun Kumar, who were constantly by my side in all difficult situations. I particularly wish to thank Mr. Rajeev Khandelwal for his help in proofreading of the manuscript and in preparing illustrations.

Finally, I wish to thank Mr. C.M. Abraham, who has typed this work with the utmost care. I think that his typing ability is fabulous by any standards.

Arun Singhal

Contents

List of figures

List of Tables

ABSTRACT

Digital protection of a power transformer is a challenging problem because of certain problems associated with transformers. These problems include magnetising inrush current, overvoltage inrush current caused by switching, tap changing provision, current transformer mismatch etc. Traditionally harmonic restraint has been used to overcome the problem of inrush currents, whereas some loss of sensitivity has been tolerated to provide for the others.

The choice of filters to be used for implementing harmonic restraint is of crucial importance for the reliable operation of the relay. It has been shown that good results can be achieved using Finite Impulse Response (FIR) filters, and Haar functions have been used to implement these.

By making provision for tap changing and using a variable bias factor, the loss of sensitivity has been minimised.

The feasibility of a drastic reduction in the hardware required for on-line, fast and reliable digital protection of a power transformer has been demonstrated. The actual hardware implementation uses a single chip microcomputer and has only 2 integrated circuits.

CHAPTER 1

INTRODUCTION

Protection of power system components has always been a challenging problem due to the inherent requirements of high reliability and fast operation of the protective equipment. These requirements are often conflicting because high reliability calls for relatively simple hardware, whereas fast operation may require more computational speed which necessitates complicated hardware. However, with the advent of VLSI technology these requirements are being reconciled more and more successfully, and exciting new possibilities in the area of protection systems are opening up.

Highly reliable relays for transmission line protection that can operate in a quarter cycle (5 ms) or less have alread been developed using travelling wave phenomenon. The same is not true for generators and transformers, which can be grouped together, because both require unit protection schemes such as percentage differential relaying, supplement by other suitable protection schemes. Most of the recent efforts to produce differential relays have been limited by computational speed requirements. In some cases, hardware multiplications and othe means requiring increased hardware have been used to facilitate computation, which lead to poorer reliability.

The availability of integrated circuits like the Intel 2920 Analog Signal Processor should make it possible soon to design differential relays on a single chip. This has been the chief motivation in inspiring this work, wherein we have investigated the possibility of making some compromises to realize this aim, and their effect on relay performance. As will be pointed out later, digital protection schemes offer several advantages over analog ones, and hence the proposed scheme is a microprocessor based, on-line digital relay.

Percentage differential relays for the protection of transformers were reported as early as 1931, by R.E. Cordray [1]. Harmonic restraint to prevent false tripping due to magnetizing inrush current was introduced soon after by Kennedy and Hayward in 1938 [2]. A relay incorporating these features and with a claimed tripping time of around 20 ms (i.e., nearly one cycle) after the occurrence of a fault was reported by Hayward in 1941 [3]. Following this, several other schemes using analog components were added to the literature on this subject [4-9], until G.D. Rockfeller came out with his landmark paper [10] in 1969, discussing the use of digital computer for, amongst various other things, transformer protection. This was followed by another paper in 1972 [11] by Sykes and Morrison, proposing a concrete scheme which could be implemented digitally and giving

simulation results to evaluate its performance. This scheme used harmonic restraint to avoid tripping due to the magnetizin inrush currents and used infinite impulse response filters to separate harmonics. The resulting scheme was slow in operation and carried with it all the drawbacks of the analog filters mimicked by it. Later attempts recognized this basic limitation and used digital filtering techniques as they emerged for various other purposes like digital signal processing, image processing, etc. In 1976, Malik, Dash and Hope proposed the use of Fourier techniques [12] for filtering purposes. Schweitzer, Larson and Flechsig used Finite Impulse Response filters [13] for this purpose. Several other papers by Degens [14], Thorp and Phadke [15], Rahman and Dash [16], discuss new ideas like rectangular transforms to minimize multiplications or computational effort, but still require complex circuitry for implementation. One of the latest papers on the subject, explores the use of Haar functions to achieve harmonic restraint [17] and proves the feasibility of such a scheme.

The study of magnetising inrush current and efficient algorithms for simulating it are essential for reliable relay design. The first detailed investigation of inrush current and the factors on which it depends was carried out by Blume et al. [19]. Detailed analysis and experiments were carried out to

determine the effect of inrush current on relaying [20]. Specht suggested some empirical expressions to simulate inrush current in a single phase transformer, in 1951 [21]. Sonnemann et al. [22] pointed out that the inrush phenomenon in three phase transformers was more complicated than single phase transformers, and some additional considerations were involved. They investigated the suitability of harmonic restraint for relaying and determined the worst possible waveforms against which any differential relay was to be tested. Several papers on inrush phenomenon in three phase transformers followed this work, including one by Specht [23]. The most recent approaches reject any functional expression for inrush current, and emphasize that a set of differential equations has to be solved numerically to simulate inrush current accurately [24].

References [25] and [26] have been used for infinite impulse response filter design in Chapter 3. References [27-30] pertain to digital signal processing and Haar function filtering. The actual hardware design has been carried out using [31] and [32].

The present work is organized into five chapters, including the present one (introduction).

In Chapter 2, the basic scheme of percentage differential protection has been introduced. The various faults possible in

a power transformer have been considered, and the scope of unit protection has been defined clearly with respect to these faults. Some problems that arise when a percentage differential relaying scheme is used to protect power transformers, like magnetizing and over-voltage inrush currents, tap changing, etc., have been discussed.

Chapter 3 is devoted entirely to the selection and design of the filters that are to be used for obtaining the fundamental component of differential and mean through currents, and the second harmonic component of the differential current. The criterion for selecting any particular filtering scheme has been to minimize settling time for a step input. Haar-function based finite impulse response filters have been chosen finally, and their performance has been examined in detail towards the end of the chapter.

The actual scheme implemented is described in detail, step-by-step, in Chapter 4. The hardware design and software used are also given therein. A good part of the chapter is devoted to evaluation of the proposed relaying scheme through simulation and actual testing of the hardware.

Finally, Chapter 5 summarizes whatever we have been able to achieve and also what we could not achieve. Our endeavour in this work was not to develop a commercial prototype, but only to demonstrate the feasibility of a drastic reduction in hardware,

while retaining the benefits of earlier designs, and perhaps improving upon them. We have succeeded in doing this, and the relay developed has been designed on a single chip. However, a lot more remains to be done, and some suggestions for future research have been given at the end of Chapter 5. The report concludes with a list of journals and books we have referred to, in the process of developing the proposed relay.

CHAPTER 2

BASIC CONCEPTS OF TRANSFORMER PROTECTION

2.1 Introductory remarks

This chapter starts with a brief description of the faults that are likely to occur in a power transformer. Protection schemes used for protecting the transformer against these faults, and also other abnormal conditions such as inrush magnetising current (which flows in the transformer when it is energised with the secondary open circuited), overexcitation inrush current (caused by overvoltages and switching) etc. have been outlined. Finally, the chapter concludes with the introduction of digital protection schemes, on-line as well as off-line, which are being explored nowadays.

2.2 Faults in a power transformer

Before attempting to discuss the protection schemes used for transformers, it is essential to enumerate the possible faults which can be encountered in a transformer. According to Warrington [18], all possible cases of abnormal operation in a transformer can be divided into two categories :

(i) External faults : This category includes problems like short duration overloading of the transformer, short circuits external to the transformer, etc. The primary transformer protection schemes should not operate in such cases. Slow blowing fuses and thermal relays are examples of the protection used against such events.

(ii) Internal faults : Faults internal to the transformer fall in two large groups, namely,

(a) Faults which can be detected by unbalance of voltage or current at the transformer terminals. These faults are of a serious nature and can cause immediate damage. Some examples of such faults are :

1) Phase to phase or phase to earth fault on the HV and LV (external) terminals.
2) Phase to phase or phase to earth fault in HV or LV windings.
3) Short circuit between turns of HV or LV winding.
4) Earth fault on a tertiary winding or short circuit between turns of a tertiary winding.

(b) Incipient faults : These faults are initially of a minor nature, and cause slowly developing damage. These faults include

1) Poor electrical connection of conductors or a core fault causing limited arcing inside oil.
2) Coolant failure.
3) Improper oil flow, allowing local hot spots to develop.
4) Regulator faults and improper load sharing between parallel transformers, causing overheating.

Some of these faults can be symbolically represented as follows :

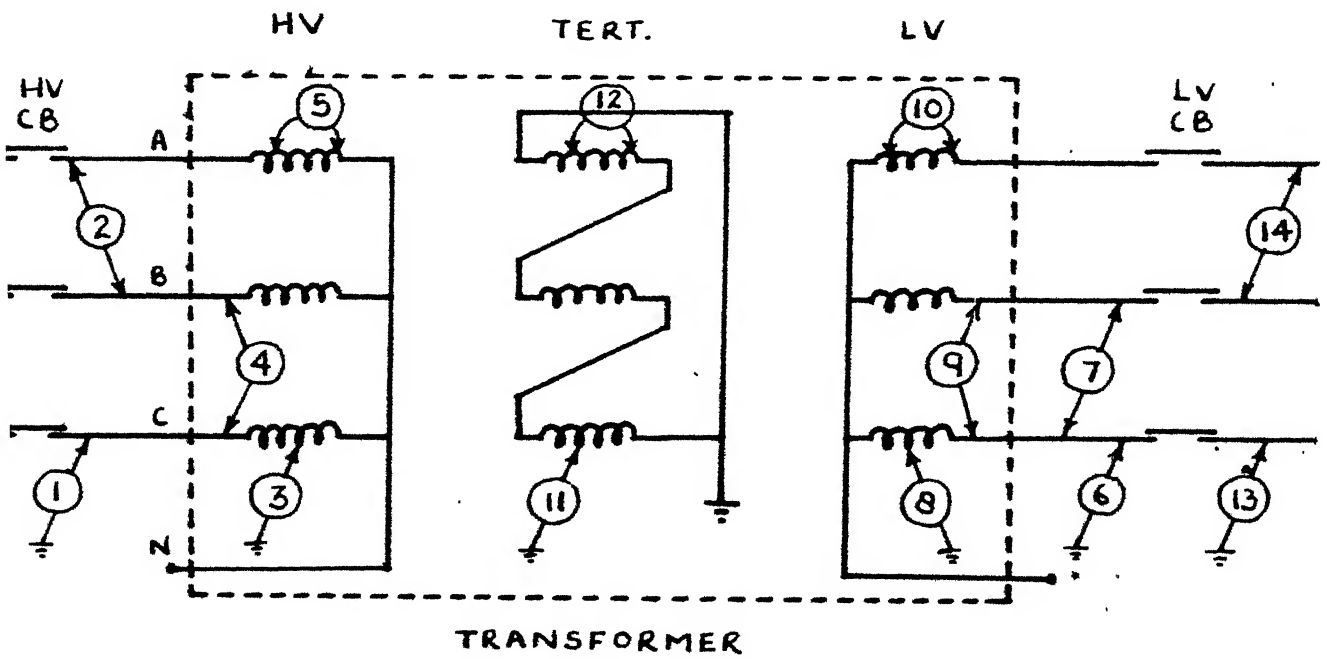

Fig. 2.1 Transformer faults

1) Earth fault on HV external connections.
2) Phase to phase fault on HV external connections.

3) Internal earth fault on HV windings.
4) Internal phase to phase fault on HV windings.
5) Short circuit between turns of HV windings.
6) Earth fault on LV external connections.
7) Phase to phase fault on LV external connections.
8) Internal earth fault on LV windings.
9) Internal phase to phase fault on LV windings.
10) Short circuit between turns of LV windings.
11) Earth fault on tertiary windings.
12) Short circuit between turns of tertiary windings.
13) Sustained system earth fault.
14) Sustained system phase to phase fault.

2.3 Protection schemes used

Group 'a' faults require fast disconnection. Relays designed for group 'a' faults will generally not operate for group 'b' faults, and relays designed for group 'b' will generally not be fast enough for group 'a' faults. Thus, protection schemes against group 'a' and group 'b' faults are not alternatives, but are supplements to each other.

Past experience has shown that gas actuated relays are adequate for group 'b' faults. The most popular gas actuated relay is the Buccholz relay, which has been used widely for several decades now.

For group 'a' faults, the use of differential protection was suggested as early as, and even before, 1931 [1]. The general idea involved in differential protection is to compare the operating quantity, which may be voltage or current, at the input and output of the equipment being protected. This comparison is a vector comparison, since the quantity being compared has a magnitude and phase associated with it. Tripping is initiated if the magnitude of the difference exceeds a predetermined constant value (or base value).

For a synchronous generator, this scheme can be implemented as shown below.

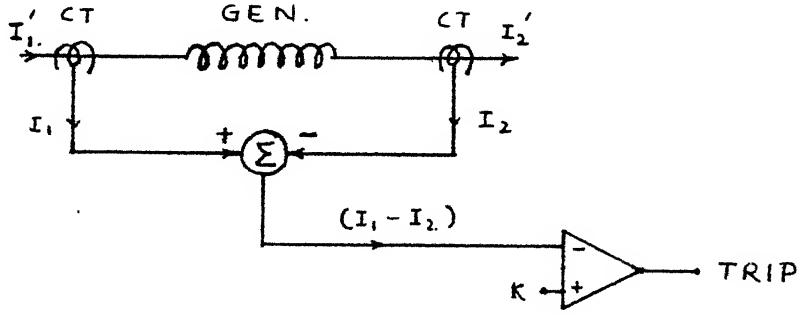

Fig. 2.2 Unit protection scheme of a synchronous generator

Both the CTs in the above scheme are identical, having the same turn ratio, and I_1' and I_2' represent the currents at the two ends of the winding. I_1 and I_2 are the scaled down versions of I_1' and I_2', respectively. Tripping occurs if

$$|\bar{I}_1 - \bar{I}_2| \geq K$$

where K is the constant base value.

There are certain problems in this scheme. At large currents due to close-by external faults, even though I_1' and I_2' are equal, I_1 and I_2 may differ significantly due to CT errors. This has led to the adoption of a modified scheme called percentage differential protection or biased differential protection, in which the magnitudes of $(\bar{I}_1-\bar{I}_2)$ and the mean through current $\frac{1}{2}(\bar{I}_1+\bar{I}_2)$ are compared. The tripping criterion now becomes

$$|\bar{I}_1-\bar{I}_2| \geq S \left| \frac{\bar{I}_1+\bar{I}_2}{2} \right|$$

where S is called the bias factor.

This scheme has been used successfully ever since the 1930s.

For a transformer, the two current transformers have to be of different turn ratios, because I_1' and I_2' are not equal for normal operation. If N_1/N_2 is the turns ratio of the power transformer being protected, then $I_1/I_2 = N_2/N_1$, if we ignore the magnetising current,which is small as compared to load currents. As a result, the turn ratios of the CTs are in the same proportion as the turns ratio of the power transformer being protected.

Further, if the winding connections of the power transformer are different on the two sides (e.g., star-delta or delta star, which is normally the case), then there will be a phase shift between the primary and secondary current. This is taken into account by connecting the CTs in the opposite way on the two sides, so that the phase shift is annulled.

All these points are illustrated in the scheme shown below:

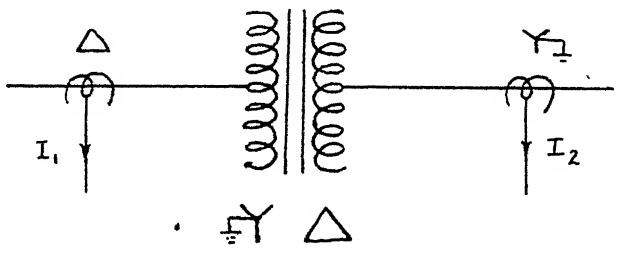

TRIP IF

$$| \bar{I}_1 - \bar{I}_2 | \geq S | \frac{\bar{I}_1 + \bar{I}_2}{2} |$$

Fig. 2.3 CT connections for protection of a Y-Δ connected transformer

Let us examine the threshold characteristic of a percentage differential relay now. Let us assume that the current $\bar{I}_1$ is the reference, i.e., $\bar{I}_1 = I_1 \angle 0^\circ$. Further, suppose $\bar{I}_2 = I_2 \angle \phi$. Then,

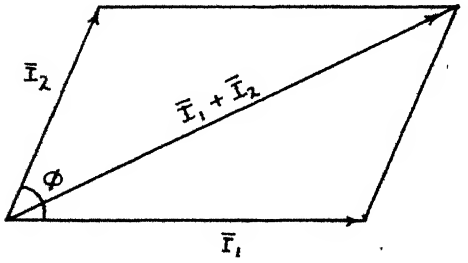

$$\bar{I}_1 + \bar{I}_2 = I_1 \angle 0 + I_2 \angle \phi$$

$$= I_1 + I_2 \cos\phi + j\, I_2 \sin\phi$$

and $$\bar{I}_1 - \bar{I}_2 = I_1 - I_2 \cos\phi - jI_2 \sin\phi$$

The threshold condition is

$$|\bar{I}_1-\bar{I}_2| = \tfrac{1}{2}\, S \;\; |\bar{I}_1+\bar{I}_2|$$

Squaring both sides, we obtain

$$|\bar{I}_1-\bar{I}_2|^2 = \tfrac{1}{4}\, S^2 \;\; |\bar{I}_1+\bar{I}_2|^2$$

Using the expressions obtained earlier, this becomes

$$(I_1-I_2\cos\phi)^2 + (I_2\sin\phi)^2 = \frac{S^2}{4}[(I_1+I_2\cos\phi)^2 + (I_2\sin\phi)^2]$$

Dividing by I_1^2 and simplifying, we obtain

$$(1-\frac{S^2}{4})(\frac{I_2}{I_1})^2 + 2(1+\frac{S^2}{4})(\frac{I_2}{I_1})\cos\phi = \frac{S^2}{4} - 1$$

Dividing by $(1-\frac{S^2}{4})$, we obtain

$$(\frac{I_2}{I_1})^2 + 2(\frac{4+S^2}{4-S^2})(\frac{I_2}{I_1})\cos\phi = -1$$

On adding $(\frac{4+S^2}{4-S^2})^2$ to both sides, this becomes

$$(\frac{I_2}{I_1})^2 + 2(\frac{I_2}{I_1})(\frac{4+S^2}{4-S^2})\cos\phi + (\frac{4+S^2}{4-S^2})^2 = (\frac{4+S^2}{4-S^2})^2 - 1 = \frac{16S^2}{(4-S^2)^2}$$

Now defining $C = \frac{4+S^2}{4-S^2}$, $r = \frac{4S}{4-S^2}$, and $\beta = \frac{I_2}{I_1}$ and substituting these, we get,

$$\beta^2 - 2\beta C \cos\phi + C^2 = r^2$$

This is the equation of a circle in polar coordinates.

The bias factor S is generally around 0.05 (5%) for synchronous generators, whereas it is kept between 0.1 and 0.4 for transformers. The reasons for using a higher value of S in the case of transformers will be discussed briefly now.

(i) Magnetising current : The primary current contains magnetising component which may be upto 5% of full load current. This current is not there on the secondary side, hence a permanent mismatch is created.

(ii) Current transformer characteristics : Usually it is not possible to find current transformers having the exact turns ratio required, since only some standardized models are available. Hence turns ratio requirements can be satisfied only approximately, and this leads to some difference in the currents being supplied to the relay even under normal conditions.

Moreover, since the current transformers employed are of different turn ratios, their cores may not get saturated by the same amount in the event of high mean through current resulting from a close by external fault. This may lead to some error in the currents being monitored.

(iii) Tap changing : Normally power transformers are provided with tap changing mechanism while CTs do not have such provision. As the transformer turns ratio is changed from the nominal value, an unbalance current flows through the differential relay.

(iv) Magnetising inrush current : To understand the phenomenon of inrush magnetising current, let us concentrate on a single-phase transformer first.

Under steady state conditions, the flux ϕ in the core of a transformer with its secondary open circuited, is in quadrature with the supply voltage waveform is as shown below.

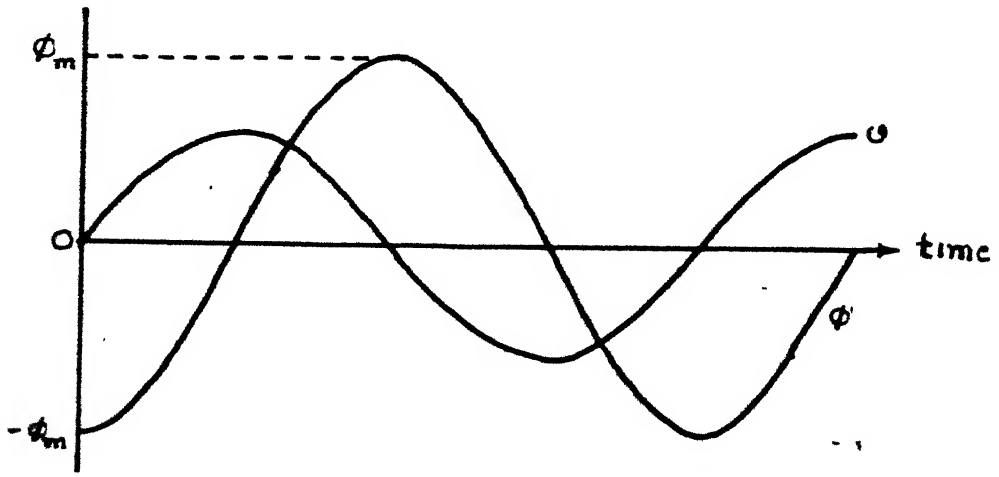

Fig. 2.4 Steady state waveforms of voltage and flux in a transformer

A sinusoidal variation of supply voltage at any instant requires a sinusoidal variation of flux in accordance with Lenz's law, i.e.,

$$v = -N \frac{d\phi}{dt}$$

where N = number of turns, t = time.

The amplitude of flux variation required for a given amplitude of supply voltage can be obtained from the steady state relationship

$$v_{rms} = 4.44 \, f\phi_{max} \, N$$

As a result, if the core has a residual flux ϕ_r before switching on, and the transformer is now switched on at any instant, the resultant flux in the core will be a sinusoidal waveshape added to a constant flux ϕ_r. To clarify this, suppose the transformer is switched on at a voltage zero. The maximum flux level attained now would by $(\phi_r \pm 2\phi_{max})$ as shown below.

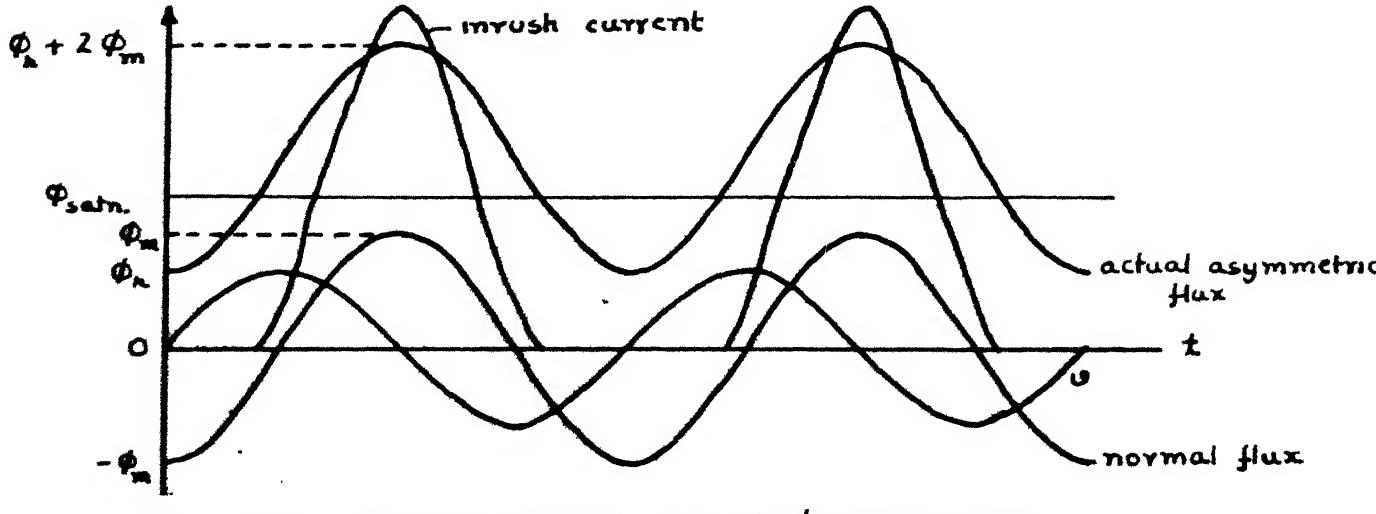

Fig. 2.5 Inrush current in a 1-ϕ transformer

Since most power transformers operate fairly close to saturation flux level, the asymmetrical flux required initially on energisation may force the core deep into saturation as depicted above. This would lead to an abnormally high requirement of magnetising current, the exact shape of which could be determined from the excitation characteristic. In fact, inrush current magnitudes of upto 15 times the rated current have been encountered.

Another problem is created by the fact that this current decays very slowly due to the large magnetising inductance of the windings, taking several seconds to decay to acceptable levels in some cases.

The phenomenon of inrush current in three phase transformers is more complicated, because the current flowing in a winding is dependent on the currents in other windings also.

The magnitude of inrush current depends on several factors such as the steel used for core construction, the level of residual magnetism as well as its polarity, the instant of switching in, and so on. Several detailed investigations have been carried out on the subject [19-24], and the phenomenon has been adequately explained for single phase as well as three phase transformers.

For relaying purposes, it is sufficient to note that the second harmonic content of an inrush current waveform is never expected to be less than 16% [22] of the fundamental, for single as well as three phase transformers. This knowledge has been used to discriminate between fault currents and inrush currents successfully for a long time and gives satisfactory results.

(v) Over voltage inrush currents : Overvoltages as high as 20 to 50% result from sudden loss of load. The magnitude of such overvoltages is determined by several factors such as generator excitation system response, the line length remaining connected to a generating station after loss of load, existence of faults preceding load rejection, system shunt reactances, total generating capacity, etc. Since modern transformers operate near saturation flux levels, such overvoltages cause a very large increase in excitation current, as large as 10 to 100 times. This increase may be sustained for long intervals, and may cause false operation of a differential relay.

An increase in magnetizing current means a large increase in the third harmonic. This could be used to recognize an overvoltage inrush current. Unfortunately, it is not always possible to monitor the third harmonic because it gets trapped inside a delta connection. The only relaying option left is to monitor

the fifth harmonic, which is also present in excitation current to a significant extent. Third harmonic monitoring would necessitate additional hardware.

The imbalance between primary and secondary current caused by the above factors even in the absence of an internal fault necessitates the use of a higher value of bias factor,s,for transformers. As hinted above, false operation due to magnetising inrush current and over-excitation inrush current caused by overvoltages/switching is prevented by monitoring the second and fifth harmonics of the differential current, respectively.

As in other fields of protection, initial differential relays designed were electro-mechanical. These relays suffered from several drawbacks, such as high burden on instrument transformers, slow operation, contact racing and contact pitting, high maintenance requirements, and false operation due to stocks or mechanical vibrations caused by external factors. With the development of electronic valves, some electro-mechanical relays were replaced by electronic ones. Electronic relays imposed low burden on instrument transformers, had no contacts or moving parts, were easy to maintain and very fast in operation, and had none of the drawbacks of electro-mechanical relays. Inspite of this, electronic relays did not find very easy acceptance, because they too had several drawbacks like

high quiescent power consumption, very high battery voltage requirement, voluminous circuitry, and uncertain life of valves.

As a result, valves were abandoned as soon as the transistor and other static components were developed. Subsequent experience showed static relays to be stable, reliable, compact in size, cheaper, and faster in operation. They can be made shock-proof and require very little maintenance and repair. They are more sensitive and permit the use of smaller CTs. More sophisticated characteristics can be realized. The only major drawbacks are complexity and change in transistor characteristic with time (aging).

Both these problems have been overcome with the introduction of digital relays. There has been an increasing tendency to use these ever since the advent of microprocessors. Initial schemes proposed the use of an off-line central digital computer for protection. More recent attempts focus on inexpensive, reliable, very fast on-line microprocessor based relays. The fact that different relay characteristics can be realized with the same hardware (or with a minimal change in hardware) adds to the charm of these relays. Moreover, fault conditions could be simulated and relay performance monitored, making these relays self checking, thus reducing maintenance and increasing reliability.

2.4 Scope of the present work

Our endeavour has been to design and fabricate an on-line percentage differential relay for transformer protection using digital signal processing techniques. The Analog Signal Processor IC Intel 2920 has been used. To define the scope of the work clearly, we must make the following clarifications at the outset :

i) Tertiary windings have been ignored.

ii) Over-voltage inrush current phenomenon has not been taken into account due to limited processing ability.

iii) Separate relays for detecting external faults, incipient faults and earth faults have been assumed.

iv) The tripping signal given is an analog output going high when tripping is required.

CHAPTER 3

FILTER DESIGN

3.1 Introduction

It was mentioned in the preceding chapter that the tripping criterion for a differential relay is given by

$$|\bar{I}_1-\bar{I}_2| \geq S\,\left|\frac{\bar{I}_1+\bar{I}_2}{2}\right|$$

Implicit in this statement was the assumption that I_1 and I_2 are sinusoidal waveforms, and hence phasors could be used to express them. However, in practice, these currents contain the fundamental component as well as several harmonics, and the resulting waveforms are periodic but non-sinusoidal. To implement the above mentioned tripping criterion, we must filter out the fundamental components of $(\bar{I}_1-\bar{I}_2)$ and $(\bar{I}_1+\bar{I}_2)$. Denoting these as $(\bar{I}_1-\bar{I}_2)_1$ and $(\bar{I}_1+\bar{I}_2)_1$, we can write the the tripping criterion as

$$|\bar{I}_1-\bar{I}_2|_1 \geq S\,\left|\frac{\bar{I}_1+\bar{I}_2}{2}\right|_1$$

This expression emphasizes the fact that we compare the rms value of the fundamental components of these currents, which is obtained after appropriate filtering.

In order to detect the inrush magnetising current, we need the second harmonic component $(\bar{I}_1-\bar{I}_2)$ as well. On the basis of results obtained by Rockfeller et al. [22], we can specify an inrush current as being the condition when

$$|\bar{I}_1-\bar{I}_2|_2 \geq 0.16\ |\bar{I}_1-\bar{I}_2|_1$$

where $(\bar{I}_1-\bar{I}_2)_2$ is the second harmonic component and $(\bar{I}_1-\bar{I}_2)$, is the fundamental component.

Combining this knowledge with the tripping criterion discussed earlier, we can write the final tripping condition as,

$$\boxed{|\bar{I}_1-\bar{I}_2|_1 \geq S\ |\frac{\bar{I}_1+\bar{I}_2}{2}|_1 \quad \text{and} \quad |\bar{I}_1-\bar{I}_2|_2 \leq 0.16\ |\bar{I}_1-\bar{I}_2|_1}$$

Clearly, such a tripping criterion would give an inrush-proof relay, i.e., a relay which would not trip due to magnetising (transient) inrush current.

The tasks to be performed can now be visualised as below :

i) Obtain samples of I_1 and I_2, convert them to digital form, and construct (I_1-I_2) and $(\frac{I_1+I_2}{2})$.

ii) Extract rms values of $(I_1-I_2)_1$, $(I_1-I_2)_2$, and $(\frac{I_1+I_2}{2})$.

iii) Test if the tripping criterion is satisfied. If yes, initiate tripping.

The relaying scheme, then, is represented by the following block diagram :

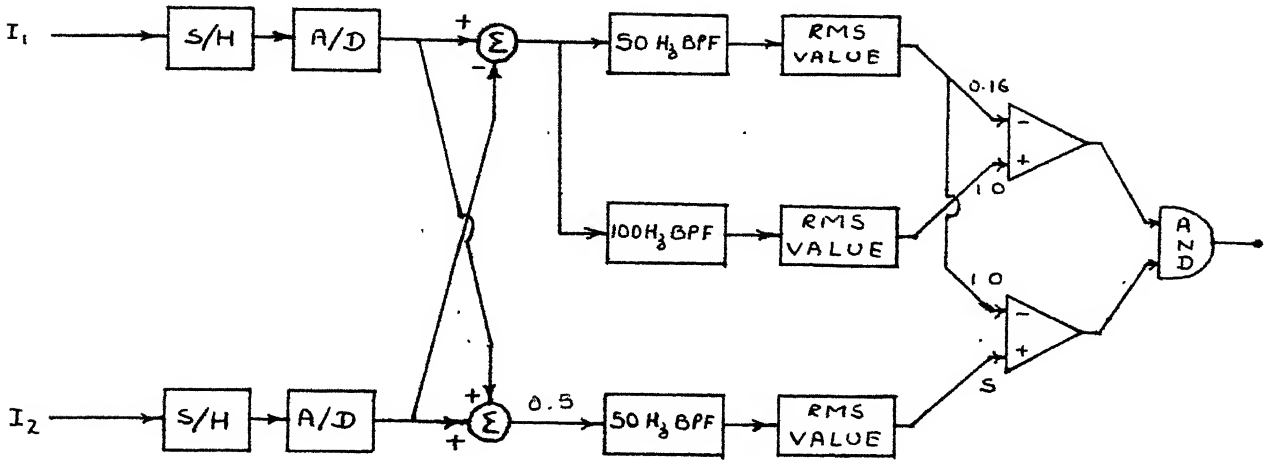

Fig. 3.1 Block diagram of a percentage differential relay

In this chapter, we shall concentrate on the design of the three filters required in the above block diagram (Fig. 3.1) After discussing their specifications, we demonstrate that infinite impulse response digital filters cannot give satisfactory results. Then we move on to the finite impulse response (FIR) digital filters and select the most suitable from amongst them, and further explore the chosen filters in some detail.

3.2 Filter specifications

It is evident that the specifications for the filters extracting $(\bar{I}_1-\bar{I}_2)_1$ and $(I_1+I_2)_1$ will be virtually identical. These filters will be referred to as the '50 Hz filters'

hereafter. The filter for extracting $(I_1-I_2)_2$ will be referred to as the '100 Hz filter'.

Let us take up the 100 Hz filter first. This filter must reject 50 Hz and 100 Hz frequencies adequately, as these are contained in the normal current as well as the fault current. How much attenuation is adequate for our purpose? To answer this, suppose (I_1-I_2) is a pure sine wave of frequency 50 Hz, having rms value equal to unity. If the 100 Hz filter attenuates 50 Hz by 20 dB, then its output will be -20 dB, or 0.1, while the 50 Hz filter gives an output of 1.0. The second harmonic is perceived as being 10% of the fundamental component, even though it is totally absent. To ensure reliable tripping, we would definitely prefer better identification of the second harmonic component.

If the 100 Hz filter attenuates 50 Hz by 30 dB, then the 'leakthrough' as calculated above will be only around 3%, which appears to be reasonably small. Let us, then, assume that we require around 30 dB attenuation of 50 Hz by the 100 Hz filter.

Since a large amount of third harmonic (150 Hz) may also be present in several cases, let us assume that the same attenuation is required for 150 Hz also. The 100 Hz filter can,

then, be specified as one which has a centre frequency of 100 Hz, and provides nearly 30 dB attenuation at 50 Hz and 150 Hz. The exact shape of the frequency response is not of any great importance to us, but all harmonics and d.c. must be attenuated sufficiently.

The constraints on the 50 Hz filter will be much less stringent, because the 50 Hz component dominates all other components of the signal in a power system. Hence, we can expect the 100 Hz filter to be the bottleneck in improving response time. Let us explore the possibility of using the infinite impulse response technique to design the 100 Hz filter, without worrying about the 50 Hz filter right now.

3.3 Choice of filtering technique

Two classes of digital filters are defined, viz: non-recursive filters, where the output is a function of only the previous and present inputs, and recursive filters, where by using feedback, the output becomes a function of past and present inputs and outputs. The non-recursive filter generates a finite impulse response and is therefore called a Finite Impulse Response (FIR) filter. Recursive filters, because of feedback, have infinite impulse responses and are referred to as Infinite Impulse Response (IIR) filters.

The traditional approach to the design of IIR digital filters involves transforming an analog filter into a digital filter that meets the prescribed specifications. This approach is useful, because the art of analog filter design is highly advanced. The conversion of an analog filter into a digital filter is accomplished in a number of ways; impulse invariance, direct transformation using s- to z-plane transforms, conversion of differential equations to difference equations, and direct synthesis. Some popular direct transforms are the matched z, left integration, Trapezoidal, Bilinear, and Prewarped Bilinear Transforms.

On the other hand, FIR filters offer several advantages. They can be designed to have exactly linear phase, thus preventing any phase distortion of the input signal. This is important for applications such as data transmission and speech processing. Due to their non-recursive structure, FIR filters are always stable. However, a strong disadvantage is that a large number of delay elements are needed to obtain a sharp cutoff, thereby requiring a large amount of processing.

Since we had limited processing ability at our disposal, we studied the possibility of using IIR filters first. Since analog filters are geometrically symmetric we can have 30 dB

attenuation (for the 100 Hz filter) at 50 Hz and $\sqrt{100^2/50}$ = 200 Hz or at 150 Hz and $\sqrt{100^2/150}$ = 66.67 Hz. The frequencies chosen are 66.67 Hz and 150 Hz for the purpose of this study. The types of filters investigated by us are Butterworth, Chebyshev, Bessel, and Legendre filters. Some others have been left out because they either appeared to have a very low cutoff rate, or had very large settling times (e.g., elliptic filters have very large settling times). The quantity of interest to us is the settling time for a step input, because we cannot take a tripping decision reliably until the filter outputs have settled down.

Table 3.1 summarizes the results of our investigation of FIR filters. From the table, it is clear that the 100 Hz filter, if designed using analog techniques cannot have a settling time less than around 3 cycles (56.2 ms).

Clearly, a Legendre filter of the fourth order gives minimum settling time. This minimum settling time (56.2 ms) is of the order of 3 cycles. If we desire tripping within a cycle after the occurrence of a fault, IIR filters will, obviously, not perform satisfactorily. Let us focus our attention on FIR filters now.

Traditional FIR filters are digital equivalents of a tapped delay line analog filter, or transversal filter. Besides

Table 3.1

Filter type	Order	3 dB BW	5% selling time
Butterworth	2	15.0	97.2
	3	25.0	74.2
	4	32.0	93.2
	5	37.5	89.8
	6	42.2	88.9
	7	45.2	107.6
Chebysehev, 0.01 dB ripple	2	15.0	56.7
	3	25.0	72.2
	4	37.5	74.1
	5	44.1	72.5
	6	50.0	71.5
	7	55.0	85.0
	8	59.0	85.9
Chebyshev, 0.1 dB ripple	2	14.4	103.2
	3	28.2	65.9
	4	38.9	75.1
	5	47.8	69.8
	6	53.6	66.4
	7	58.1	83.5
Bessel	2	12.5	112.3
	3	18.7	82.4
	4	21.4	78.8
	5	25.0	72.7
	6		77.3
Legendre	2	13.3	62.1
	3	27.3	62.0
	4	37.7	56.2
	5	45.7	72.0
	6	51.9	69.9
	7	56.9	80.4

Table 3.1 A comparison of various analog filters with centre frequency 100 Hz and 30 dB attenuation points at 66.67 Hz and 150 Hz. Data obtained from references [25] and [26]

requiring a large number of delay elements (memory locations) they require a lot of computational effort because of the weighing factors involved. Since multiplication is a time consuming operation, a simple hardware realization of such filters becomes difficult.

Another option left open is to use any one of the transform domains employed in image processing. A brief comparison of these transforms is given in Table 3.2, which has been reproduced partly from [27].

A Fourier transform would give the harmonic amplitudes directly. If we use any other transform and wish to obtain the harmonic contents, some subsequent processing will be required. Even so, the table 3.2 indicates that Haar transform achieves such a drastic reduction in computational effort that there may be a reduction in the overall effort required. This is borne out by previous attempts using FFT [12] and Haar transform [17].

In view of the facts mentioned above, it will be desirable to use Haar transform for filtering what follows is a brief review of Haar functions and their use in digital filtering.

3.4 Haar transform-based filters

The Haar functions form a complete set of orthogonal rectangular functions. They were established by the Hungarian

Table 3.2

Transform Domains for Coding

Transform name	Order of computations
Singular value decomposition	$4N^3$
Karhunen-Loeve Hotelling, principal components, factor analysis	$2N^3$
Cosine	$2N^2\log_2 N$
Fourier	$2N^2\log_2 N$ (complex)
Slant	$2N^2\log_2 N$
DLB	$2N^2\log_2 N$ (integer)
Walsh	$2N^2\log_2 N$ (additions)
Haar	$2(N-1)$ (additions)
Hybrid	$N^2\log N + nN^2$ *
DPCM	$2nN^2$ *

te : For the entries marked with an asterisk (*), n is proportional to the order of predictor used. N is the number of samples for slant, Walsh, Haar; $N = 2^k$ where k is an integer. For cosine, Fourier, DLB; order of computations is more than the estimate given if $N \neq 2^k$ with k being an integer.

mathematician Alfred Haar in a paper published in 1910 [28]. He described a set of orthogonal functions, each taking essentially two values, and yet providing an expansion of a given continuous function, which could be made to converge rapidly and uniformly. This was a property not obtainable by any other set of non-sinusoidal orthogonal functions at that time. However, very little practical use was made of these functions for over half a century until the 1960s, when they were seen to provide some computational advantages in certain areas of communication, image coding, and digital filtering.

If we consider a time base $0 \leq t \leq t$, then we can define Haar functions as,

$$HAR(2^p+n,t) = \begin{cases} \sqrt{2^p} & \text{for } \frac{n}{2}\, p \leq t \leq (n+\frac{1}{2})/2^p \\ -\sqrt{2^p} & \text{for } (n+\frac{1}{2})/2^p \leq t \leq (n+1)/2^p \\ 0 & \text{elsewhere .} \end{cases}$$

The first 8 Haar functions are shown in Fig. 3.2.

It can be shown from the definition that

$$\int_0^1 HAR(m,t)\, HAR(n,t)dt = \begin{cases} 1 & \text{for } n = m \\ 0 & \text{for } n \neq m \end{cases}$$

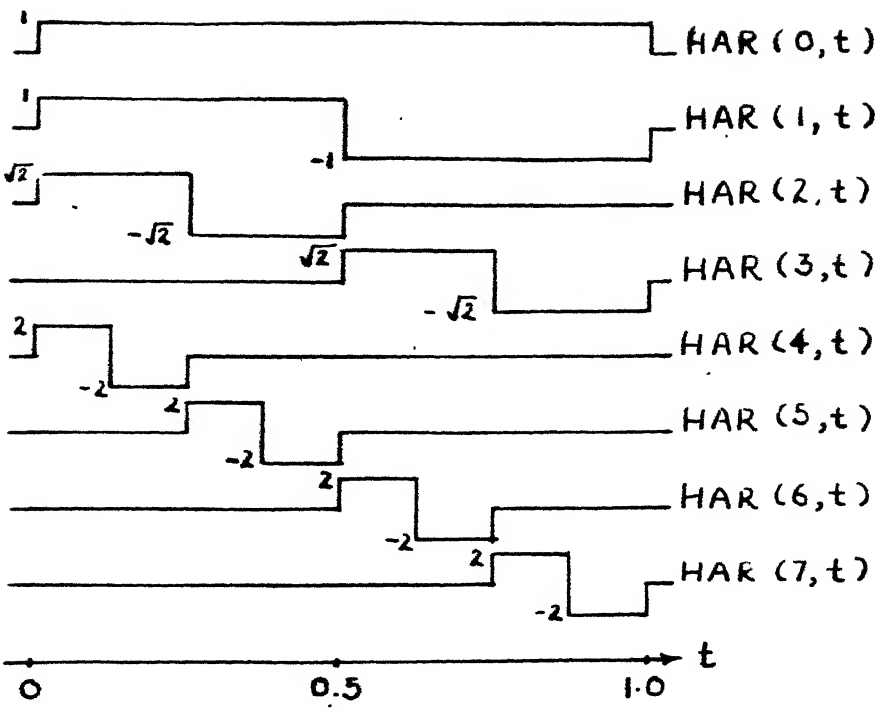

Fig. 3.2 The first 8 Haar functions

This constitutes the property of orthogonality. The proof of completeness is given by Haar [28]. Thus, Haar functions as defined above form a complete set of orthogonal functions.

Any given continuous function, periodic with a time period T = 1, can be synthesized from a Haar series by

$$f(t) = \sum_{n=0}^{\infty} C_n \, HAR(n,t) \qquad (3.1)$$

where

$$C_n = \int_0^1 f(t) \times HAR(n,t) \, dt \qquad (3.2)$$

The convergence features of Haar series have been examined by Alexits [29]. It has been shown by Shore [30], that, a comparatively small number of terms is necessary to approximate a waveform using the Haar series.

If a function f(t) is specified by N samples $(X_1, X_2, \ldots, X_N)$ during a time period, we cannot use a Haar series for it. However, we can define the discrete Haar transform and its inverse from equations (3.1) and (3.2) as,

$$X_n = \frac{1}{N} \sum_{i=0}^{N-1} C_i \; HAR\,(n, i/N)$$

$$C_i = \sum_{n=0}^{N-1} X_n \; HAR\,(n, i/N)$$

$$i,n = 0,1,2, \ldots, N-1$$

Written in the matrix form, these equations become,

$$[X]_{Nx1} = \frac{1}{N} [H]_{NxN} [C]_{Nx1} \tag{3.3}$$

and

$$[C]_{Nx1} = [H]^{-1}_{Nx1} [X]_{Nx1} \tag{3.4}$$

where [H] is the Haar function matrix and $[H]^{-1}$ is its inverse. $[H]^{-1}$ is simply given by the transpose of [H], because of the orthogonality property. For N = 8, the matrix [H] would be

$$[H]=\begin{bmatrix} 1 & 1 & 1 & 1 & 1 & 1 & 1 & 1 \\ 1 & 1 & 1 & 1 & -1 & -1 & -1 & -1 \\ \sqrt{2} & \sqrt{2} & \sqrt{2} & \sqrt{2} & 0 & 0 & 0 & 0 \\ 0 & 0 & 0 & 0 & \sqrt{2} & \sqrt{2} & \sqrt{2} & \sqrt{2} \\ 2 & -2 & 0 & 0 & 0 & 0 & 0 & 0 \\ 0 & 0 & 2 & -2 & 0 & 0 & 0 & 0 \\ 0 & 0 & 0 & 0 & 2 & -2 & 0 & 0 \\ 0 & 0 & 0 & 0 & 0 & 0 & 2 & -2 \end{bmatrix} \qquad (3.5)$$

If this transformation is carried out directly, N^2 operations are required. However, if a factorization algorithm similar to the one used for fast Fourier Transform is used, the total number of operations can be reduced to 2(N-1). A flow diagram for the 8 point fast Haar Transform is shown in Fig. 3.3. The solid lines show addition and the dotted lines show subtraction at the nodal points. The multiplications have all been delayed until the transformation is complete.

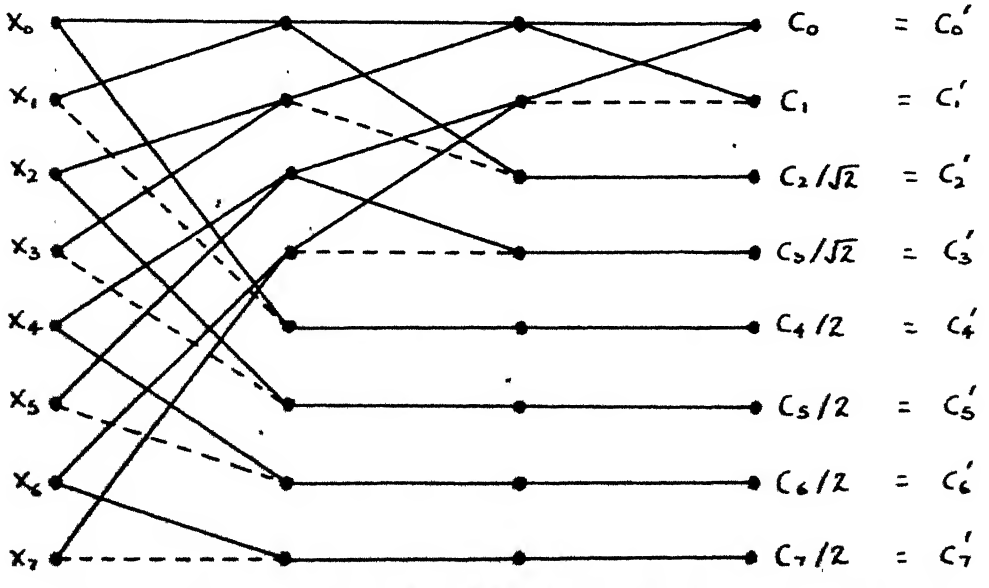

Fig. 3.3 Flow diagram for an 8 point Fast Haar Transform

Once the Haar coefficients have been determined using the above scheme, the Fourier series coefficients can be obtained as derived below :

$$\text{Let } f(t) = F_o + \sqrt{2}F_1 \sin \frac{2\pi}{T} t + \sqrt{2} F_2 \cos \frac{2\pi}{T} t + \ldots$$

$$+ \sqrt{2}F_3 \sin \frac{4\pi}{T} t + \sqrt{2}F_4 \cos \frac{4\pi}{T} t + \ldots$$

We can assume, without any loss of generality, that the fundamental time period T = 1. The coefficients $F_1, F_2, \ldots$ are given by

$$F_1 = \sqrt{2} \int_0^1 f(t) \sin 2\pi t \, dt$$

$$F_2 = \sqrt{2} \int_0^1 f(t) \cos 2\pi t \, dt \qquad (3.6)$$

$$\vdots \qquad\qquad \vdots$$

Now $f(t) = \sum_{n=0}^{\infty} C_n \, HAR(n,t)$. It follows from equation (3.6) that

$$F_1 = \sqrt{2} \int_0^1 \left[\sum_{n=0}^{\infty} C_n \, HAR(n,t) \right] \sin 2\pi t \, dt$$

$$= \sqrt{2} \left[C_o \int_0^1 \sin 2\pi t \, dt + C_1 . 2 . \int_0^{1/2} \sin 2\pi t \, dt + \ldots \right]$$

$$= 0.9C_1 + 0.1865 \, (-C_4 + C_5 + C_6 + C_7) + \ldots$$

If we are using the discrete Haar transform with N = 8, we obtain,

$$F_1 = 0.9C_1 + 0.1865\ (-C_4+C_5+C_6-C_7)$$

$$F_2 = 0.6366(C_2-C_3)+0.1865(C_4+C_5-C_6-C_7)$$

$$F_3 = 0.6366\ (C_2+C_3)$$

$$F_4 = 0.6366(C_4-C_5+C_6-C_7)$$

If we define modified Haar coefficients as indicated in Fig. 3.3, these expressions get modified to,

$$F_1 = 0.9C_1' + 0.373\ (C_5'+C_6'-C_4'-C_7')$$

$$F_2 = 0.9(C_2'-C_3') + 0.373(C_4'+C_5'-C_6'-C_7') \qquad (3.7)$$

$$F_3 = 0.9(C_2'+C_3')$$

$$F_4 = 0.9(C_4'-C_5'+C_6'-C_7')$$

The rms values of the first and the second harmonic are given by

$$A_1 = \sqrt{F_1^2 + F_2^2}$$
$$A_2 = \sqrt{F_3^2 + F_4^2} \qquad (3.8)$$

The frequency response of the filters so obtained is shown in Table 3.3. 8 point Fast Haar Transformation has been used. The response is plotted in Fig. 3.4. The response is such that all undesirable frequencies will be rejected adequately if the operating frequency is exactly 50 Hz. With change in frequency, the degradation of performance is severe.

Table 3.4 presents the simulated step response of Haar function filters. The results are plotted in Fig. 3.5(b). The settling time is clearly less than 20 milliseconds. Table 3.5 and Fig. 3.5(a) show the simulated impulse response. The response to a centre frequency step input is shown for both filters in Figures 3.5(c) and 3.5(d), and the simulated data in Tables 3.6 and 3.7.

3.5 Conclusion

In this chapter, we have shown the feasibility and attractiveness of using Haar transform based filters for differential relaying. In the next one, we shall discuss the actual scheme that has been implemented.

Table 3.3

Frequency Response

Frequency (Hz)	50 Hz filter output (per unit)	100 Hz filter outp (per unit)
0.0	0.0000	0.0000
5.0	0.1912	0.0948
10.0	0.3341	0.1611
15.0	0.4010	0.1799
20.0	0.4073	0.1494
25.0	0.4299	0.0932
30.0	0.5465	0.0832
35.0	0.7245	0.1266
40.0	0.8844	0.1415
45.0	0.9728	0.0992
46.0	0.9799	0.0835
47.0	0.9834	0.0656
48.0	0.9835	0.0456
49.0	0.9803	0.0237
50.0	0.9741	0.0000
51.0	0.9651	0.0252
52.0	0.9537	0.0517
53.0	0.9402	0.0793
54.0	0.9251	0.1078
55.0	0.9087	0.1367
60.0	0.8232	0.2809
65.0	0.7626	0.4031
70.0	0.7317	0.4877
75.0	0.6935	0.5431
80.0	0.6112	0.5996
85.0	0.4755	0.6829
90.0	0.3053	0.7842
95.0	0.1351	0.8677
96.0	0.1042	0.8790
97.0	0.0751	0.8880
98.0	0.0479	0.8946
99.0	0.0228	0.8985
100.00	0.0000	0.8999
101.00	0.0204	0.8985
102.0	0.0384	0.8946
.03.0	0.0537	0.8880
.04.0	0.0666	0.8790
.05.0	0.0769	0.8677
.10.0	0.0969	0.7842
.15.0	0.1000	0.6829
.20.0	0.1436	0.5996
.25.0	0.2064	0.5431
.30.0	0.2445	0.4877
.35.0	0.2358	0.4031
.40.0	0.1797	0.2809
.45.0	0.0923	0.1367
.50.0	0.0002	0.0000
.55.0	0.0705	0.0992

Frequency (Hz)	50 Hz filter output (per unit)	100 Hz filter output(per unit)
160.0	0.0993	0.1415
165.0	0.0816	0.1266
170.0	0.0328	0.0832
175.0	0.0571	0.0932
180.0	0.1167	0.1494
185.0	0.1464	0.1799
190.0	0.1327	0.1611
195.0	0.0785	0.0949
200.0	0.0000	0.0000

Table 3.3 Frequency response of Haar function based filters

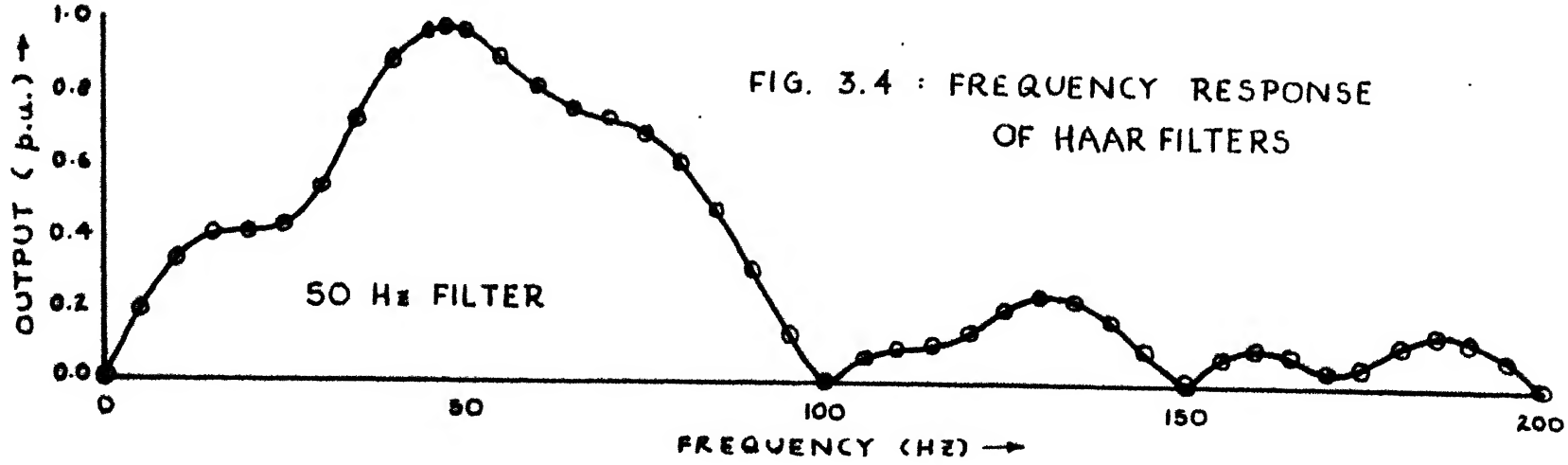

FIG. 3.4 : FREQUENCY RESPONSE OF HAAR FILTERS

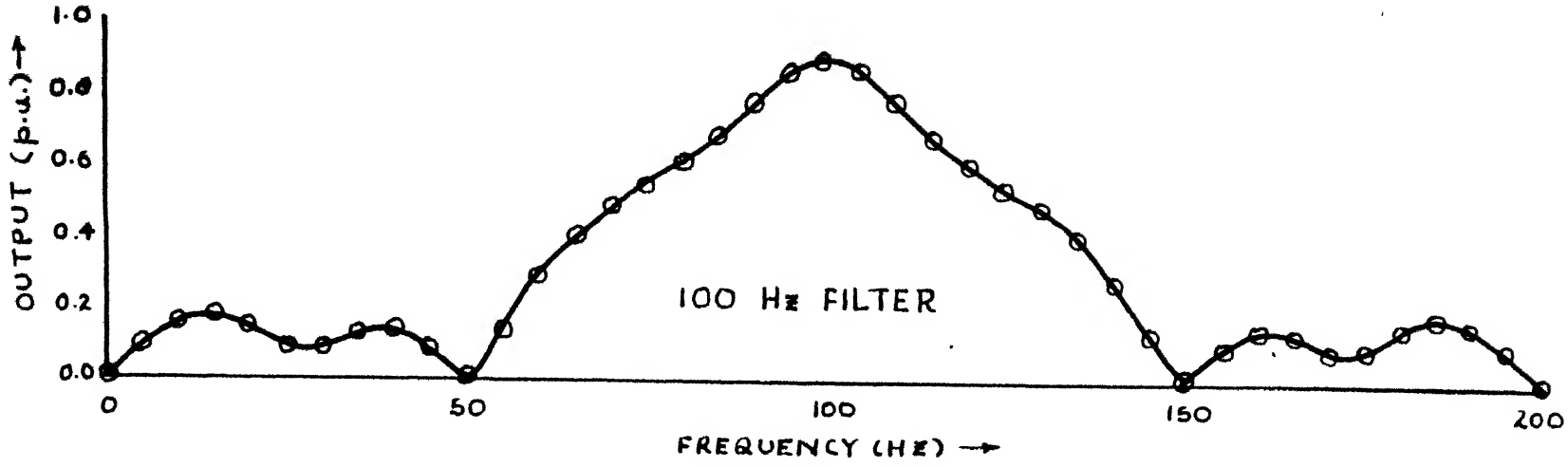

Table 3.4

Time (ms)	Input	50 Hz filter	100 Hz filt
0.00	1.00	0.17	0.16
2.50	1.00	0.32	0.22
5.00	1.00	0.42	0.16
7.50	1.00	0.45	0.00
10.00	1.00	0.42	0.16
12.50	1.00	0.32	0.22
15.00	1.00	0.17	0.16
17.50	1.00	0.00	0.00
20.00	1.00	0.00	0.00
22.50	1.00	0.00	0.00
25.00	1.00	0.00	0.00
27.50	1.00	0.00	0.00
30.00	1.00	0.00	0.00
⋮			
50.00	1.00	0.00	0.00

Table 3.4 Step response

Table 3.5

Time (ms)	Input	50 Hz filter	100 Hz filte
0.00	1.00	0.17	0.16
2.50	0.00	0.17	0.16
5.00	0.00	0.17	0.16
7.50	0.00	0.17	0.16
10.00	0.00	0.17	0.16
12.50	0.00	0.17	0.16
15.00	0.00	0.17	0.16
20.00	0.00	0.00	0.00
22.50	0.00	0.00	0.00
25.00	0.00	0.00	0.00
27.00	0.00	0.00	0.00
30.00	0.00	0.00	0.00
.			
.			
.			
50.00	0.00	0.00	0.00

Table 3.5 Impulse response

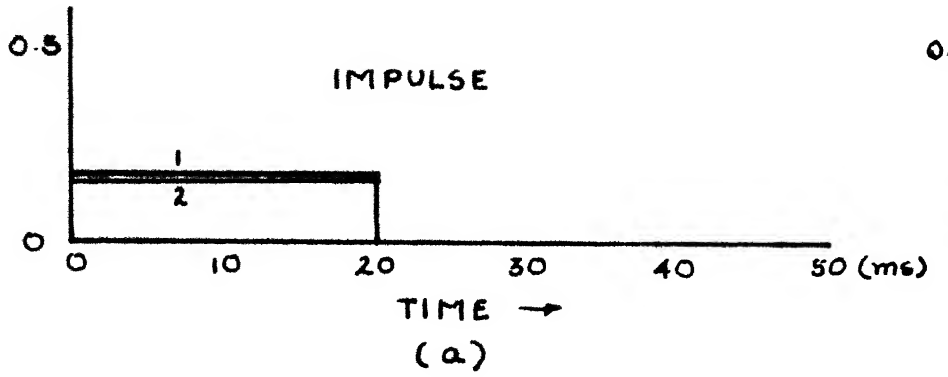

(a)

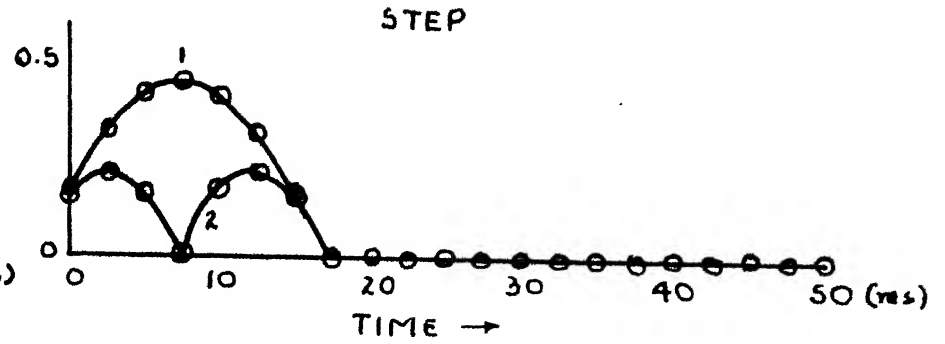

(b)

FIG. 3.5 : TIME RESPONSE OF HAAR FILTERS

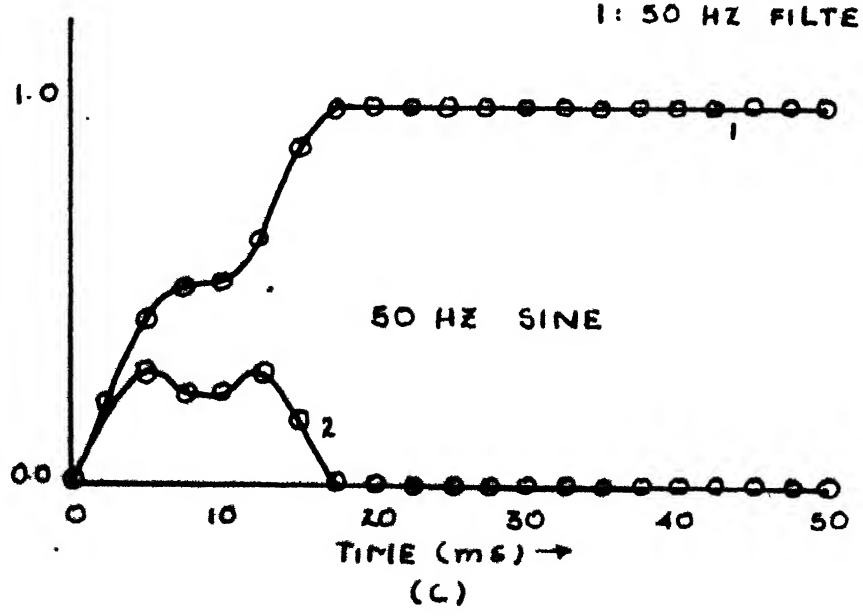

(c)

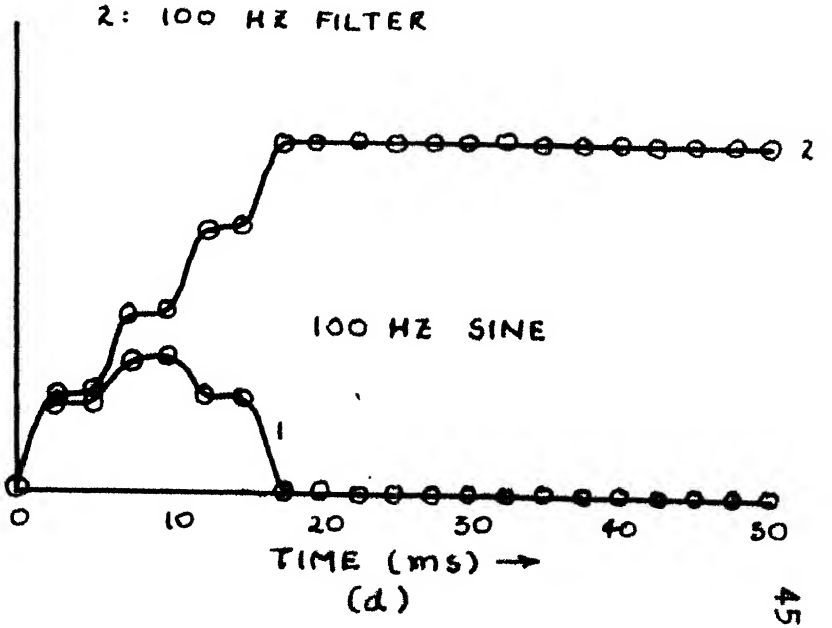

(d)

Table 3.6

Time (ms)	Input	50 Hz filter	100 Hz filter
0.00	0.00	0.00	0.00
2.50	1.00	0.17	0.16
5.00	1.41	0.39	0.28
7.50	1.00	0.49	0.22
10.00	0.00	0.49	0.22
12.50	-1.00	0.62	0.28
15.00	-1.41	0.86	0.16
17.50	-1.00	0.97	0.00
20.00	0.00	0.97	0.00
22.50	1.00	0.97	0.00
25.00	1.41	0.97	0.00
27.50	1.00	0.97	0.00
30.00	0.00	0.97	0.00

Table 3.6 50 Hz sine wave step response

Table 3.7

Time (ms)	Input	50 Hz filter	100 Hz filter
0.00	0.00	0.00	0.00
2.50	1.41	0.24	0.22
5.00	0.00	0.24	0.22
7.50	-1.41	0.34	0.45
10.00	0.00	0.34	0.45
12.50	1.41	0.24	0.67
15.00	0.00	0.24	0.67
17.50	-1.41	0.00	0.90
20.00	0.00	0.00	0.90
22.50	1.41	0.00	0.90
25.00	0.00	0.00	0.90
27.50	-1.41	0.00	0.90
30.00	0.00	0.00	0.90

Table 3.7 100 Hz sine wave step response

CHAPTER 4

PROPOSED SCHEME

4.1 Introduction

In the previous chapters, we have discussed the general requirements of a differential relay for transformer protection. Some partial solutions of the problems encountered were also discussed. This chapter describes the actual integrated solution that has been implemented to overcome most of the difficulties envisaged, and presents the results of some realistic studies carried out to determine the performance of the proposed relaying scheme. It has been shown that the relay fabricated would function satisfactorily even in the worst possible conditions. The limitations of the relay developed are also brought out.

The flexibility and comprehensiveness of the proposed relaying scheme is limited by the abilities of the 2920 Analog Signal Processor. This single chip microcomputer has been designed especially to process real time analog signals. It has on-board program memory, scratchpad memory, D/A circuitry, A/D circuitry, digital processor, and I/O circuitry. It can execute programs upto 13,000 times a second if the entire

program memory of 192 instructions is used, which allows processing of signals upto 5 kHz bandwidth. With shorter programs, the processing speed can be increased further.

While the presence of so many features on a single chip greatly helps in simplifying hardware requirements, it generates limitations on the actual performance and ability of each facility provided. For example, whereas the 2920 can handle upto 4 analog inputs and 8 analog outputs simultaneously, it takes around 40 instructions for each analog input operation (which can be carried out side-by-side with other computations) and around 12 instructions for each analog output operation in a typical hardware configuration used. This, coupled with some other constraints, makes it virtually impossible to use all the inputs and outputs simultaneously. This prevented us from outputting the operating and restraining signals.

The most severe limitation faced was of program and scratchpad memory limitation. The 2920 has only 192 instructions program memory and 40 RAM locations as scratchpad memory. If we try to compute 16 sample Haar transforms of primary and secondary currents, then 32 RAM locations are required just for storing samples of both these currents, and it is not possible to perform all other computations using just 8 memory locations. As a result, we were limited to 8 sample Haar transforms, which

are inadequate for extracting the 5th harmonic component. This forced us to drop over-voltage inrush detection facility in the scheme. Some other compromises were also necessary, and they will gradually become clear as we describe the implemented scheme step-by-step. Let us, then, move on to a description of what has been achieved.

4.2 Description of the scheme

4.2.1 Input

The currents I_1 and I_2, obtained from the current transformers, are first converted into voltages by passing them through suitable air core transactors. After this, they are sampled by the relay.

The two currents are sampled within 50 microseconds of each other in the proposed scheme.

4.2.2 Tap changing

To account for the mismatch created by tap changing in a power transformer, one of the sampled currents is multiplied by a correction factor. Besides I_1 and I_2, a third analog input indicating the tap setting is provided to the relay. The value of this third input TAP can be varied between +1.0 and -1.0, and the correction factor used is (1+TAP/8). In other words, samples of I_1 are replaced by I_1 (1+TAP/8). With this provision,

tap setting changes upto $\pm 12.5\%$ from the nominal value can be accounted for.

4.2.3 Filtering

As mentioned in the introductory remarks, 8 sample Haar transforms have been used. First of all, the mean through current $(\frac{I_1+I_2}{2})$, and (I_1-I_2) to provide operating signals, are obtained from I_1 (corrected for tap setting) and I_2. After this, these are passed through filters to obtained $(\frac{I_1+I_2}{2})$, (I_1-I_2), and $(I_1-I_2)_2$. These three signals have been designated restraining (RES), operating (OP) and inrush (INR) signals respectively.

While implementing equations (3.7) using 2920, it is of great advantage if the coefficients of C_o', ..., C_1' can be written as sums and differences of a small number of terms involving powers of 2. For instance, the binary representation of 0.875 is 0.111, which means $0.875 = 2^{-1}+2^{-2}+2^{-5}$. However, if we recognize that $0.875 = 1-0.125 = 1-2^{-3}$, we can implement this coefficient in a smaller number of instructions. Therefore, equations (3.7) have been modified as given below :

$$
\begin{aligned}
F1 &= 0.90625\ C_1' + 0.375\ (C_5'+C_6'-C_4'-C_7') \\
F2 &= 0.9023(C_2'-C_3') + 0.375(C_4'+C_5'-C_6'-C_7') \\
F3 &= 0.9023(C_2'+C_3') \\
F4 &= 0.9023(C_4'-C_5'+C_6'-C_7')
\end{aligned}
\qquad (4.1)
$$

Due to the change in the values of coefficients, the frequency response of the filters changes slightly. Table 4.1 and Fig. 4.0 show the modified frequency response.

4.2.4 RMS value computation

According to equations (3.8), the rms values of the fundamental and second harmonic contents are given by

$$A_1 = \sqrt{F_1^2 + F_2^2}$$
$$A_2 = \sqrt{F_3^2 + F_4^2} \qquad (3.8)$$

These equations require squaring and square rooting operations, which require very large computational efforts. To avoid this, an approximation is being employed.

Suppose, we want to compute $\theta = \sqrt{x^2+y^2}$ and x and y are both positive. Since both of these appear squared in the expression for θ, their polarity (sign) is not really important and we can use their absolute values (i.e. modulus). Consequently, we can confine out attention to the first quadrant of the x-y plane.

The first quadrant is further divided into two zones by the line L (x = y) shown in Fig. 4.1. In region I, $x \geq y$, whereas in region II, $y \geq x$.

Table 4.1

Frequency (Hz)	50 Hz Filter output (p.u.)	100 Hz Filter output (p.u.)
0.0	0.0000	0.0000
5.0	0.1925	0.0951
10.0	0.3364	0.1615
15.0	0.4037	0.1804
20.0	0.4096	0.1498
25.0	0.4315	0.0934
30.0	0.5482	0.0834
35.0	0.7273	0.1269
40.0	0.8886	0.1419
45.0	0.9782	0.0995
46.0	0.9854	0.0837
47.0	0.9891	0.0658
48.0	0.9893	0.0457
49.0	0.9862	0.0237
50.0	0.9801	0.0000
51.0	0.9712	0.0253
52.0	0.9598	0.0519
53.0	0.9463	0.0795
54.0	0.9311	0.1080
55.0	0.9147	0.1371
60.0	0.8285	0.2816
65.0	0.7669	0.4042
70.0	0.7348	0.4890
75.0	0.6958	0.5445
80.0	0.6130	0.6012
85.0	0.4769	0.6847
90.0	0.3062	0.7862
95.0	0.1354	0.8700
96.0	0.1045	0.8813
97.0	0.0753	0.8903
98.0	0.0481	0.8969
99.0	0.0229	0.9009
100.0	0.0000	0.9022
101.0	0.0205	0.9009
102.0	0.0385	0.8969
103.0	0.0539	0.8903
104.0	0.0668	0.8813
105.0	0.0772	0.8700
110.0	0.0972	0.7862

115.0	0.1004	0.6847
120.0	0.1439	0.6012
125.0	0.2068	0.5445
130.0	0.2447	0.4890
135.0	0.3259	0.4042
140.0	0.1794	0.2816
145.0	0.0917	0.1371
150.0	0.0011	0.0000
155.0	0.0715	0.0995
160.0	0.1002	0.1419
165.0	0.0823	0.1269
170.0	0.0333	0.0834
175.0	0.0576	0.0934
180.0	0.1174	0.1498
185.0	0.1472	0.1804
190.0	0.1335	0.1615
195.0	0.0789	0.0951
200.0	0.0000	0.0000

Table 4.1 Frequency response of Haar filters used (Input waveform has unity rms value)

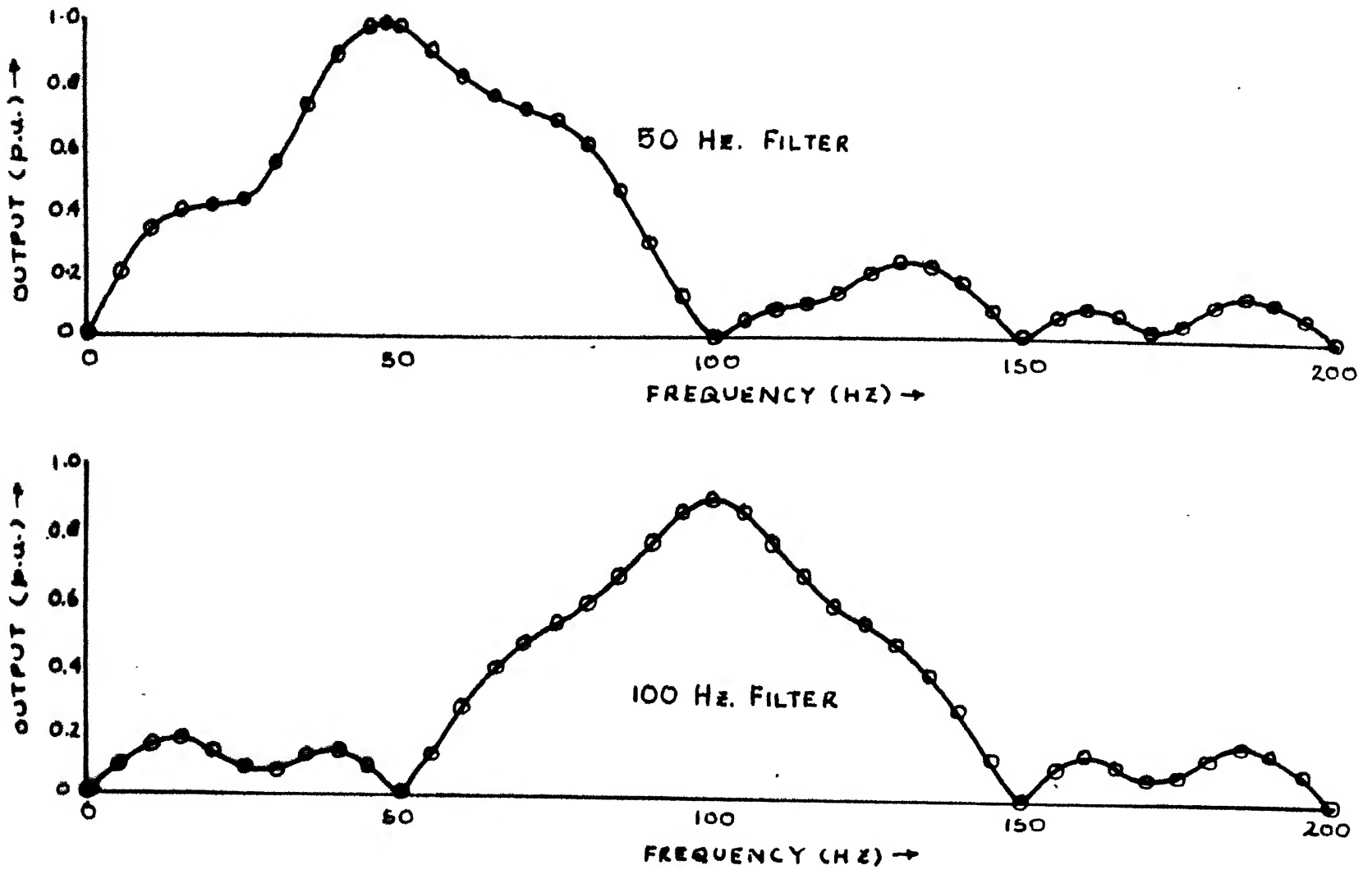

FIG. 4.0 : FREQUENCY RESPONSE OF HAAR FILTERS OBTAINED

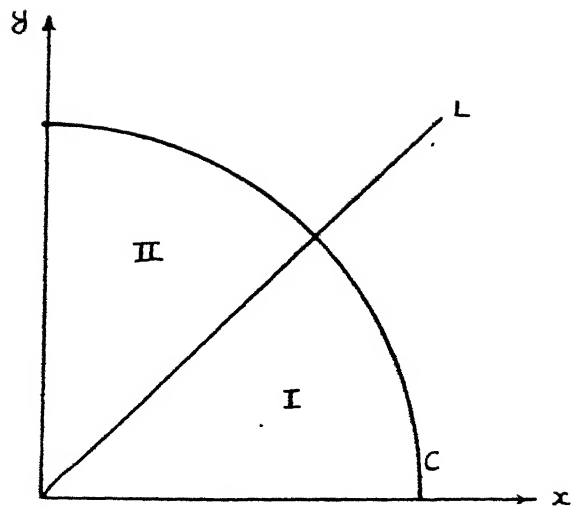

Fig. 4.1

Consider an estimator of the form $\theta = Ax + By$ in the region I. Without any loss of generality, we may assume that (x,y) lie on the unit circle $x^2+y^2 = 1$ (curve c) for the purpose of determining the accuracy of this estimator, since any other combination of (x,y) can be obtained merely by scaling them. The error in the estimated value is given by,

$$= (Ax + By) - 1 \qquad (\because\ x^2+y^2 = 1)$$

At which point on c does this error become maximum? To answer this, let us switch over to polar coordinates and redefine error as,

$$f(\theta) = (A\cos\theta + B\sin\theta) - 1$$

On differentiating with respect to θ, we obtain

$$f'(\theta) = -A \sin\theta + B \cos\theta$$

Therefore, $f'(\theta) \Rightarrow A \sin\theta = B \cos\theta \Rightarrow \tan\theta = B/A$

In region I, $0 \leq \theta \leq 45^\circ$, or $0 \leq \tan\theta \leq 1$. This means that A and B are of the same sign (positive), and $B \leq A$, if $f(\theta)$ is to have an extremum in region I.

The second derivative $f''(\theta) = (-A \cos\theta - B \sin\theta)$ is non-positive in the region I. This means that $f(\theta)$ attains a maximum at $\theta = \tan^{-1}(B/A)$, and the maximum error is found to be,

$$f(\theta)_{max} = \sqrt{A^2+B^2}-1$$

All these results can be summarized as given below :

Objective function : $\theta = \sqrt{x^2+y^2}$, for $x \geq y \geq 0$

Estimator used : $\theta = AX + BY$, with $A \geq B \geq 0$.

θ	Error	Comments
0°	$A-1$	
45°	$\frac{A+B}{\sqrt{2}} - 1$	
$\tan^{-1}(B/A)$	$\sqrt{A^2+B^2} - 1$	Maximum error

We want to find A,B such that error is reasonably small in the entire region I.

Since we are constrained to select values which are easily realizable, we have chosen A = 1 and B = 1/2. For these values, the estimator always overestimates the objective function, the extent of overestimation varying from 0% to 11.8% to 6.07% as θ varies from 0° to 26.56° to 45° respectively. Better estimators are, of course, possible. For example, A = 1 and B = $\sqrt{2}-1$ (= 0.414) gives a maximum error of +8.24% only; and A = 0.95, B = 0.464 gives maximum errors of -5% and $+5.735^\circ$ only. However, as pointed out earlier, A = 1 and B = 0.5 are easy to implement.

Using this estimator, equations (3.8) get modified to the following form :

$$A_1 = \max(|F_1|, |F_2|) + \tfrac{1}{2} \min(|F_1|, |F_2|)$$
$$A_2 = \max(|F_3|, |F_4|) + \tfrac{1}{2} \min(|F_3|, |F_4|) \qquad (4.2)$$

These equations give rise to a maximum error of 11.8% in the ratio A_1/A_2 (not 23.6% because both the errors can be positive only). This error has to be absorbed in the margin of safety in the tripping criterion.

4.2.5 Variable bias factor

The problems of CT mismatch etc. are less severe when the

currents I_1 and I_2 are small. This means that we can use a smaller value of bias factor S when the mean through current $(\frac{I_1+I_2}{2})$ is small, leading to more sensitive relaying. However, S has to be increased as the mean through current becomes larger and the CTs begin to get saturated.

We have used a bias factor which is directly proportional to the mean through current and is given by

$$S = (\frac{I_1+I_2}{2})_{rms} + 0.0625 \qquad (4.3)$$

It is to be noted that for the relay developed, S can vary between 0.0625 and nearly 0.77 under the worst possible conditions. For normal load currents, S will be nearly 0.10 to 0.72.

4.3 Hardware description

The hardware configuration used has been taken from the 2920 Analog Signal Processor Design Handbook [31] and is shown in Fig. 4.2.

Fig. 4.3 shows the PCB layout used, and Fig. 4.4 shows a photograph of the complete relay. The relay requires +5V and -5V power supplies, and has no provision for input conditioning.

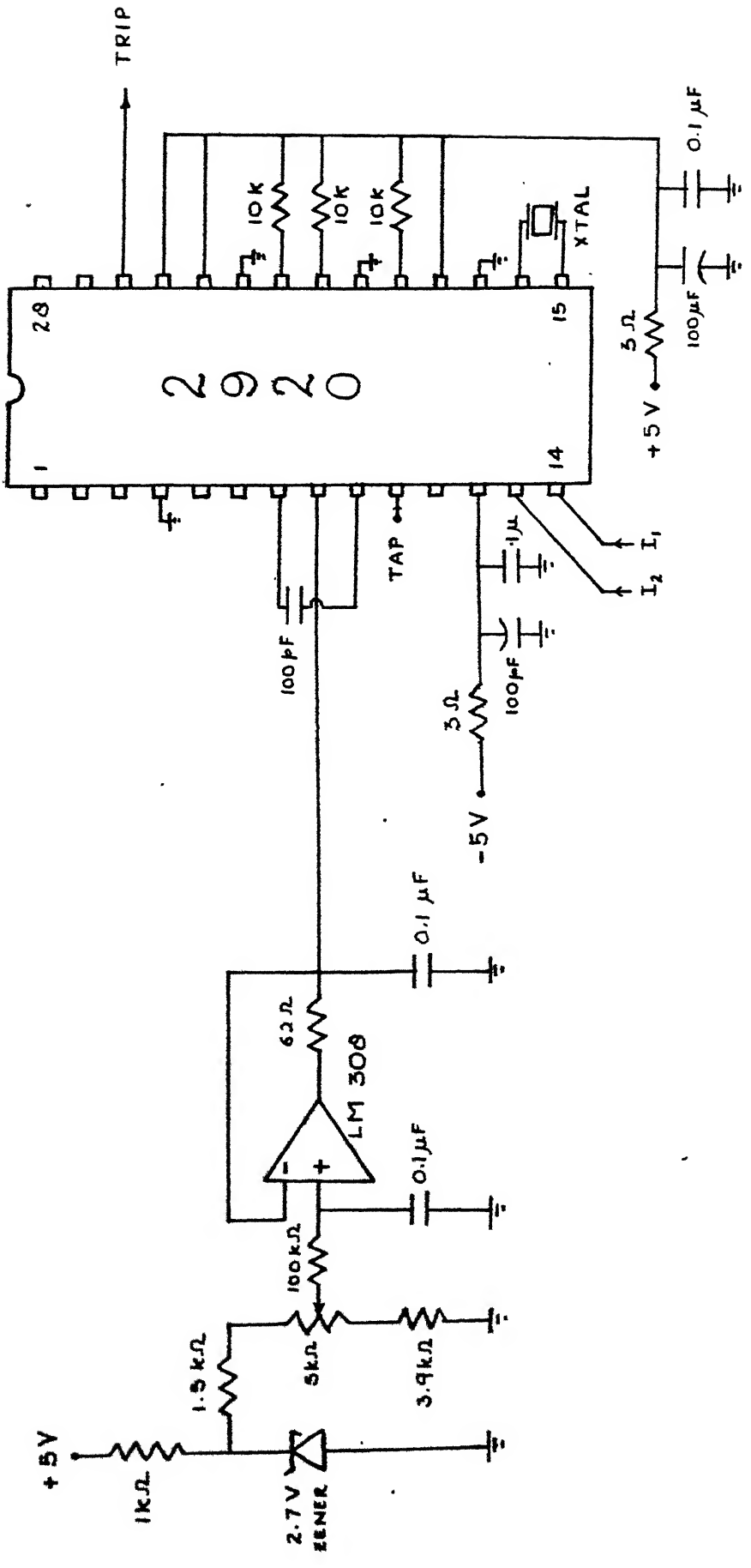

Fig. 4.2 Circuit diagram of the relay

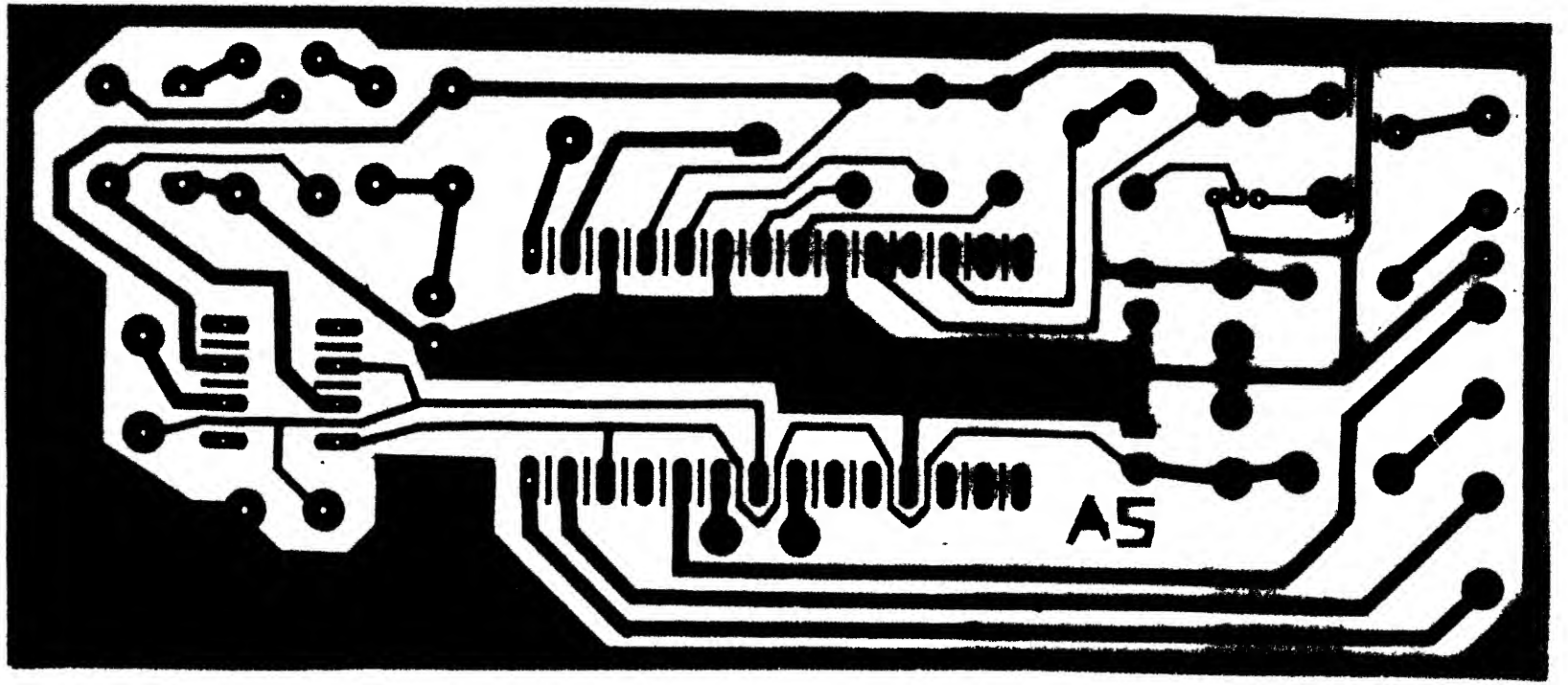

Fig. 4.3 PCB layout of the relay

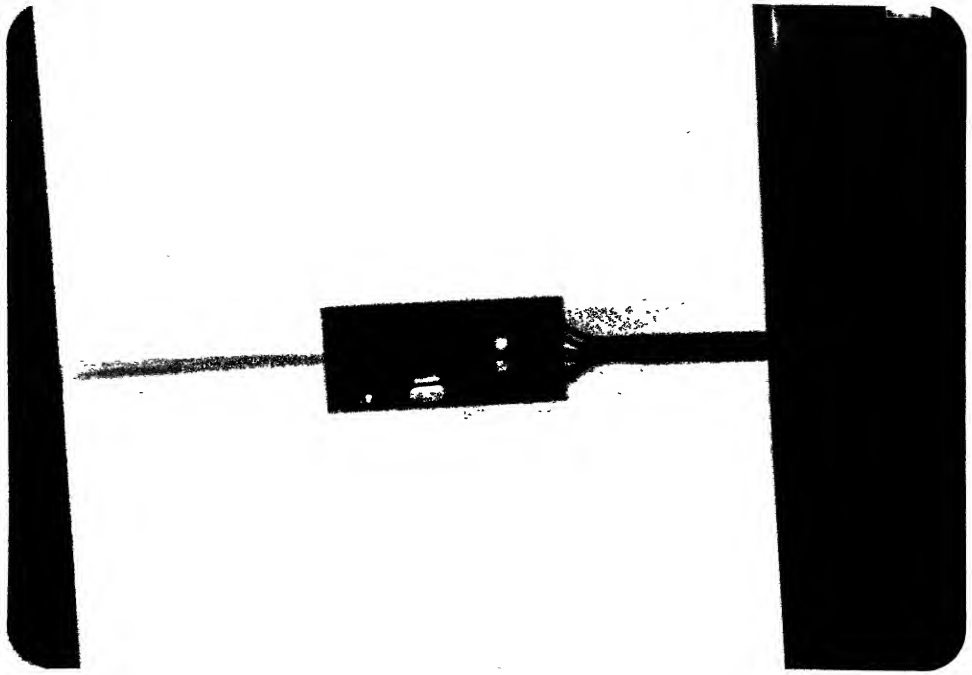

Fig. 4.4 Photograph of the relay which has been developed

4.4 Software used

Table 4.2 gives the complete assembly language program listing used. The details and basic facts about 2920, as well as information about the assembly language, can be obtained from [31].

4.5 Performance of the proposed scheme

The steady state tripping characteristic of a percentage differential relay is a circle as shown in Chapter 2 (Section 2.3). Such a characteristic is obtained only if the bias factor S is a constant. For the proposed scheme, wherein S varies with the mean through current, any such characteristic cannot be obtained. We can only study a few cases and verify if all provisions work as stipulated.

The other aspect that needs to be tested is the transient response, i.e., how soon does the relay trip after the occurrence of a fault and how do the operating, inrush, and restraining signals vary in the meantime. The actual hardware developed would provide only one output - the trip signal, hiding much relevant information. Therefore, we have used a software package SM2920, which was developed by Intel Corporation to simulate the performance of 2920 software. The use of this simulator allows us to monitor signals internal to the relay, which would be 'invisible' in the hardware.

Table 4.2

```
ROM 000 = LDA DAR . CTR. R00, NOP
ROM 001 = SUB DAR, KP1, R02, NOP
ROM 002 = LDA . CTR. KP6, R00, CND5
ROM 003 = SUB DAR. DAR, R00, IN0
ROM 004 = LDA . C0, . N0, R00, IN0
ROM 005 = ADD . C0, . N1, R00, IN0
ROM 006 = LDA . C1, . N2, R00, IN0
ROM 007 = ADD . C1, . N3, R00, IN0
ROM 008 = LDA . C6, . N4, R00, IN0
ROM 009 = ADD . C6, . N5, R00, NOP
ROM 010 = LDA . C7, . N6, R00, NOP
ROM 011 = ADD . C7, . N7, R00, CVT5
ROM 012 = LDA . C4, . C0, R00, NOP
ROM 013 = ADD . C4, . C1, R00, NOP
ROM 014 = LDA . C5, . C6, R00, CVT7
ROM 015 = ADD . C5, . C7, R00, NOP
ROM 016 = LDA . C2, . C0, R00, NOP
ROM 017 = SUB  C2, . C1, R00, CVT6
ROM 018 = LDA . C3. . C6, R00, NOP
ROM 019 = SUB . C3,  C7, R00, NOP
ROM 020 = LDA . C1, . C4, R00, CVT5
ROM 021 = SUB . C1, . C5, R00, NOP
ROM 022 = LDA  C4, . N0, R00, NOP
ROM 023 = SUB . C4, . N1, R00, CVT4
ROM 024 = LDA . C5, . N2, R00, NOP
ROM 025 = SUB . C5, . N3, R00, NOP
ROM 026 = LDA . C6, . N4, R00, CVT3
ROM 027 = SUB  C6, . N5. R00, NOP
ROM 028 = LDA  C7, . N6, R00, NOP
ROM 029 = SUB . C7, . N7, R00, CVT2
ROM 030 = LDA . F1, . C5, R01, NOP
ROM 031 = ADD . F1, . C6, R01, NOP
ROM 032 = SUB . F1, . C4, R01, CVT1
ROM 033 = SUB . F1, . C7, R01, NOP
ROM 034 = SUB . F1, . F1, R02, NOP
ROM 035 = ADD . F1, . C1, R00, CVT0
ROM 036 = SUB . F1, . C1, R03, NOP
ROM 037 = ADD . F1, . C1, R05, NOP
ROM 038 = LDA . TAP, DAR, R06, NOP
ROM 039 = SUB DAR, DAR, R00, IN1
ROM 040 = LDA . F2, . C4, R01, IN1
ROM 041 = ADD . F2, . C5, R01, IN1
ROM 042 = SUB . F2, . C6, R01, IN1
ROM 043 = SUB . F2, . C7, R01, IN1
ROM 044 = SUB . F2, . F2, R02, IN1
ROM 045 = SUB . C2, . C2, R03, NOP
ROM 046 = SUB . C3, . C3, R03, NOP
ROM 047 = ADD . C2, . C2, R05, CVT5
```

contd..

```
ROM 048 = ADD  C3,  C3, R05, NOP
ROM 049 = ADD  F2,  C2, R00, NOP
ROM 050 = SUB  F2,  C3, R00, CVT7
ROM 051 = LDA . F3, . C2, R00, NOP
ROM 052 = ADD . F3, . C3, R00, NOP
ROM 053 = LDA . F4, . C4, R00, CVT6
ROM 054 = SUB . F4,  C5, R00, NOP
ROM 055 = ADD . F4,  C6, R00, NOP
ROM 056 = SUB  F4, . C7, R00, CVT5
ROM 057 = SUB . F4,  F4, R03, NOP
ROM 058 = ADD . F4, . F4, R05, NOP
ROM 059 = LDA . C0, . M0, R00, CVT4
ROM 060 = ADD . C0,  M1, R00, NOP
ROM 061 = LDA . C1, . M2, R00, NOP
ROM 062 = ADD . C1, . M3, R00, CVT3
ROM 063 = LDA  C6, . M4, R00, NOP
ROM 064 = ADD . C6, . M5, R00, NOP
ROM 065 = LDA . C7, . M6, R00, CVT2
ROM 066 = ADD . C7, . M7, R00, NOP
ROM 067 = LDA . C4, . C0, R00, NOP
ROM 068 = ADD . C4, . C1, R00, CVT1
ROM 069 = LDA . C5, . C6, R00, NOP
ROM 070 = ADD . C5, . C7, R00, NOP
ROM 071 = LDA . C2, . C0, R00, CVT0
ROM 072 = SUB . C2, . C1, R00, NOP
ROM 073 = LDA . C3, . C6, R00, NOP
ROM 074 = LDA . I1, DAR, R03, NOP
ROM 075 = ADD . I1, . TAP, R01, CND7
ROM 076 = ADD . I1, . TAP, R02, CND6
ROM 077 = ADD . I1, . TAP, R03, CND5
ROM 078 = ADD . I1, . TAP, R04, CND4
ROM 079 = ADD . I1, . TAP, R05, CND3
ROM 080 = ADD . I1, . TAP, R06, CND2
ROM 081 = ADD . I1, . TAP, R07, CND1
ROM 082 = ADD . I1, . TAP, R08, CND0
ROM 083 = SUB . TAP, . TAP, L01, NOP
ROM 084 = ADD . I1, . TAP, R00, CND8
ROM 085 = SUB DAR, DAR, R00, IN2
ROM 086 = SUB . C3, . C7, R00, IN2
ROM 087 = LDA . C1, . C4, R00, IN2
ROM 088 = SUB . C1, . C5, R00, IN2
ROM 089 = ABS . OP, . F1, L01, IN2
ROM 090 = ABA . OP, . F2, R00, IN2
ROM 091 = ABS . F2, . F2, R00, NOP
ROM 092 = ABA . F2, . F1, R01, NOP
ROM 093 = ABS . INR, . F3, R00, CVT8
ROM 094 = ABA . INR, . F4, R01, NOP
ROM 095 = ABS . F4, . F4, R00, NOP
```

contd..

```
ROM 096 = ABA  F4,  F3,R01,CVT7
ROM 097 = LDA . C4,  M0,R01,NOP
ROM 098 = SUB  C4,  M1,R01,NOP
ROM 099 = SUB . C4,. M4,R01,CVT6
ROM 100 = ADD  C4,  M5,R01,NOP
ROM 101 = LDA . C5,. M2,R01,NOP
ROM 102 = SUB . C5 . M3,R01,CVT5
ROM 103 = SUB . C5,. M6,R01,NOP
ROM 104 = ADD . C5,. M7,R01,NOP
ROM 105 = SUB  C4,. C4,R02,CVT4
ROM 106 = SUB . C5,. C5,R02,NOP
ROM 107 = LDA . F1,  C1,R00,NOP
ROM 108 = SUB . F1,. F1,R03,CVT3
ROM 109 = ADD . F1,. F1,R05,NOP
ROM 110 = SUB . F1,. C4,R00,NOP
ROM 111 = ADD . F1,. C5,R00,CVT2
ROM 112 = LDA . F3,. C2,R00,NOP
ROM 113 = SUB . F3,. C3,R00,NOP
ROM 114 = SUB . F3,. F3,R03,CVT1
ROM 115 = ADD . F3,. F3,R05,NOP
ROM 116 = ADD . F3,. C4,R00,NOP
ROM 117 = ADD . F3,. C5,R00,CVT0
ROM 118 = ABS . AVG,. F1,R00,NOP
ROM 119 = ABA . AVG,. F3,R01,NOP
ROM 120 = ABS . F3,. F3,R00,NOP
ROM 121 = ABA . F3,. F1,R01,NOP
ROM 122 = LDA . TAP,. I1,R01,NOP
ROM 123 = ADD . TAP,DAR,R04,NOP
ROM 124 = SUB . I1,DAR,R03,NOP
ROM 125 = ADD . CTR,KP1,R02,NOP
ROM 126 = LDA DAR,KP6,R00,NOP
ROM 127 = SUB DAR. DAR,R06,NOP
ROM 128 = SUB DAR,. CTR,R00,NOP
ROM 129 = LDA . CTR,KP1,R00,CNDS
ROM 130 = LDA . N0,. N1,R00,CNDS
ROM 131 = LDA . N1,  N2,R00,CNDS
ROM 132 = LDA . N2,. N3,R00,CNDS
ROM 133 = LDA . N3,. N4,R00,CNDS
ROM 134 = LDA . N4,. N5,R00,CNDS
ROM 135 = LDA . N5,. N6,R00,CNDS
ROM 136 = LDA . N6,. N7,R00,CNDS
ROM 137 = LDA . M0,. M1,R00,CNDS
ROM 138 = LDA . M1,. M2,R00,CNDS
ROM 139 = LDA . M2,. M3,R00,CNDS
ROM 140 = LDA . M3,. M4,R00,CNDS
ROM 141 = LDA . M4,. M5,R00,CNDS
ROM 142 = LDA . M5,. M6,R00,CNDS
ROM 143 = LDA . M6,. M7,R00,CNDS
```

contd..

```
ROM 144 = LDA . N7, . TAP, R00, CND7
ROM 145 = LDA . N7, . I1, R01, CND6
ROM 146 = ADD . N7, . OLD, R01, CND5
ROM 147 = SUB . I1, . I1, L01, NOP
ROM 148 = LDA . OLD, . I1, R00, CND5
ROM 149 = LDA DAR, . OP, R00, NOP
ROM 150 = SUB DAR, . F2, L01, NOP
ROM 151 = LDA . OP, . F2, L01, CND5
ROM 152 = ADD . OP, . OP, R02, NOP
ROM 153 = LDA DAR, . AVG, R00, NOP
ROM 154 = SUB DAR, . F3, R00, NOP
ROM 155 = LDA . AVG, . F3, R00, CND5
ROM 156 = LDA DAR, . INR, R00, NOP
ROM 157 = SUB DAR, . F4, R00, NOP
ROM 158 = LDA . INR, . F4, R00, CND5
ROM 159 = ADD . INR, . INR, R01, NOP
ROM 160 = LDA DAR, . AVG, R00, NOP
ROM 161 = ADD DAR, KP1, R01, NOP
ROM 162 = ADD . RES, . AVG, R01, CND7
ROM 163 = ADD . RES, . AVG, R02, CND6
ROM 164 = ADD . RES, . AVG, R03, CND5
ROM 165 = ADD . RES, . AVG, R04, CND4
ROM 166 = ADD . RES, . AVG, R05, CND3
ROM 167 = ADD . RES, . AVG, R06, CND2
ROM 168 = ADD . RES, . AVG, R07, CND1
ROM 169 = ADD . RES, . AVG, R08, CND0
ROM 170 = SUB . AVG, . AVG, L01, NOP
ROM 171 = ADD . RES, . AVG, R00, CND5
ROM 172 = SUB . OP, KP1, R05, NOP
ROM 173 = LDA . TRIP, KP7, R00, NOP
ROM 174 = LDA DAR, . OP, R01, NOP
ROM 175 = SUB DAR, . INR, L02, NOP
ROM 176 = LDA . TRIP, KP0, R00, CND5
ROM 177 = LDA DAR, . OP, R00, NOP
ROM 178 = SUB DAR, . RES, R00, NOP
ROM 179 = LDA . TRIP, KP0, R00, CND5
ROM 180 = LDA DAR, . TRIP, R00, NOP
ROM 181 = LDA . TAP, . RES, R00, NOP
ROM 182 = SUB . RES, . RES, R00, NOP
ROM 183 = SUB . AVG, . AVG, L01, NOP
ROM 184 = LDA . CTR, . CTR, R00, NOP
ROM 185 = LDA . CTR, . CTR, R00, NOP
ROM 186 = LDA . CTR, . CTR, R00, OUT0
ROM 187 = LDA . CTR, . CTR, R00, OUT0
ROM 188 = LDA . CTR, . CTR, R00, OUT0
ROM 189 = LDA . CTR, . CTR, R00, OUT0
ROM 190 = LDA . CTR, . CTR, R00, OUT0
ROM 191 = LDA . CTR, . CTR, R00, OUT0
WRITE TO.
```

Table 4.2 Software developed for the relay

The transient response has been tested for three different inputs, representing severe internal fault current, worst case one-phase inrush current, and worst case three-phase inrush current.

Table 4.3 and Fig. 4.5 show the results for simulated fault conditions in an unloaded single-phase transformer. Data to represent samples of differential current in this situation were obtained from

$$I_1 = \sin(\omega t - \gamma) - e^{-(\omega t - \theta)/Q} \sin(\theta - \gamma)$$

where $\gamma = \arctan Q$

$Q = \omega L/R$

Values of $Q = 10$ and $\theta = 0$ were used to obtain the fault waveform. It was also assumed that $I_2 = 0$, because the fault occurs on an unloaded transformer. This approach has been adapted from [11].

The results indicate that the tripping command was issued within a cycle (17.75 ms), and there were no significant variations in the internal variables after this. The tripping criterion were satisfied with a very large margin.

The next input considered was that of inrush current in a single phase transformer. Modelling of this current follows the approach suggested in [22], and samples to represent i_1 were obtained from

Table 4.3

Time (ms)	Input	OP	INR	RES	TRIP
0.25	0.000	-0.039	0.000	0.000	0.002
2.75	0.034	0.018	0.317	0.001	0.002
5.25	0.102	0.157	0.780	0.007	0.002
7.75	0.160	0.278	0.766	0.018	0.002
10.25	0.170	0.270	0.608	0.031	0.002
12.75	0.123	0.348	0.885	0.030	0.002
15.25	0.044	0.534	0.806	0.032	0.002
17.75	-0.025	0.666	0.277	0.032	0.877
20.25	-0.045	0.643	0.000	0.041	0.877
22.75	-0.008	0.675	0.039	0.042	0.877
25.25	0.062	0.648	0.039	0.043	0.877
27.75	0.124	0.691	0.039	0.040	0.877
30.25	0.137	0.663	0.039	0.036	0.877
32.75	0.092	0.684	0.000	0.032	0.877
35.25	0.015	0.644	0.039	0.032	0.877
37.75	-0.052	0.675	0.039	0.035	0.877
40.25	-0.070	0.647	0.000	0.039	0.877
42.75	-0.030	0.673	0.000	0.041	0.877
45.25	0.042	0.654	0.039	0.041	0.877
47.75	0.104	0.684	0.039	0.038	0.877
50.25	0.119	0.655	0.000	0.037	0.877

Table 4.3 Simulated results for relay operation during a fault

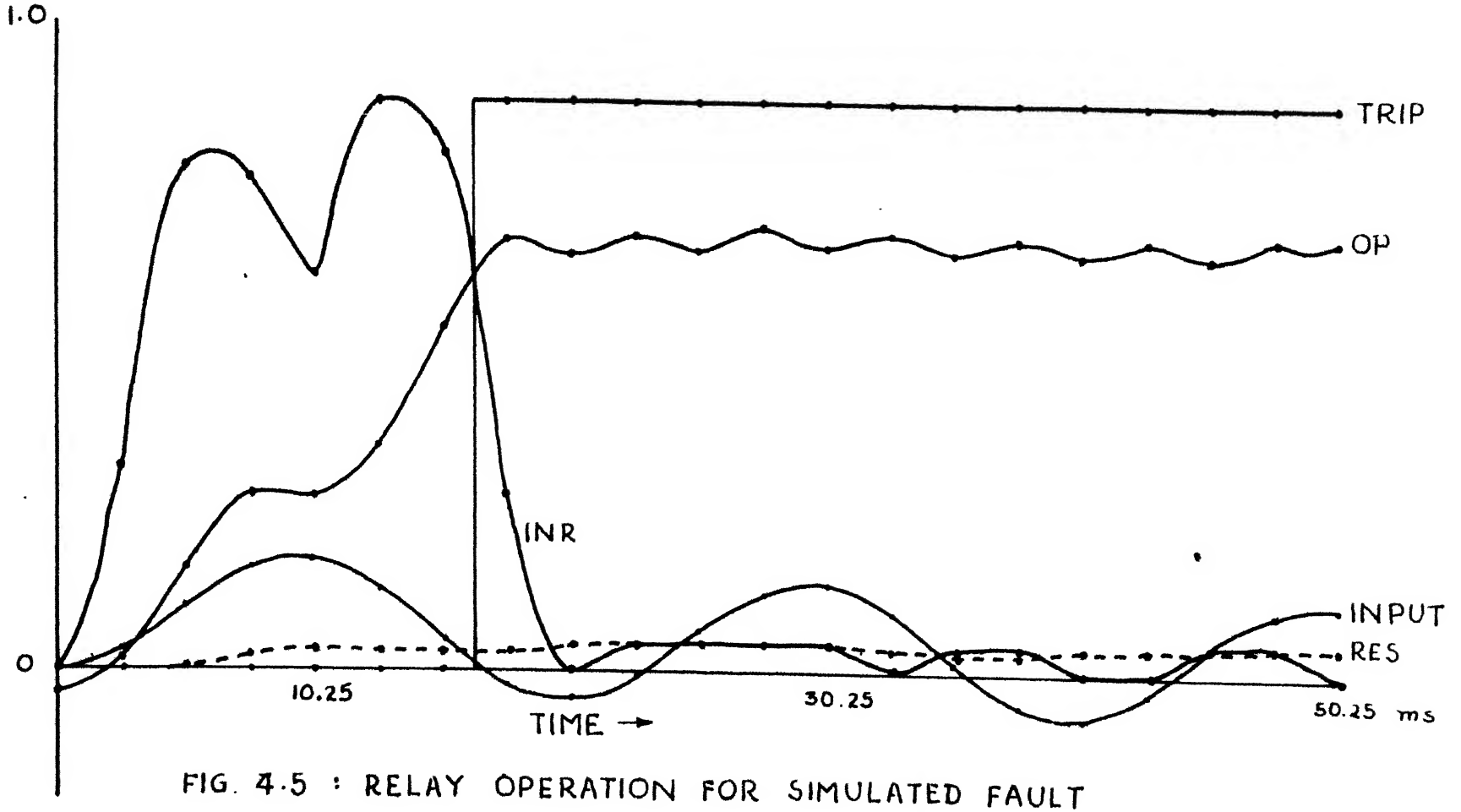

FIG. 4.5 : RELAY OPERATION FOR SIMULATED FAULT

$$i_1 = \text{POS}\ (0.5 - \cos \omega t)$$

where POS (x) = x if $x \geq 0$, and 0 otherwise.

This waveform corresponds to a residual flux density of 0.9 p.u. and a saturation flux density of 1.4 p.u. It has been assumed that the transformer is switched in at 0° in the voltage cycle, as this corresponds to the maximum inrush current. It has been verified [22] that this waveform has the minimum ontainable amount of second harmonic (17.1%) for any residual flux level. I_2 was assumed to be zero.

The results are given in Table 4.4 and Fig. 4.6. Again, we find that all internal variables stabilize within a cycle, and tripping is avoided by a comfortable margin for this worst case single phase inrush current.

The worst inrush current waveform for a three phase transformer (for the purpose of relaying) has been taken to be

$$i_1 = \text{POS}\ (0.5 - \cos \omega t) + \text{POS}\ (\sin (\omega t - 30^\circ))$$

and $i_2 = 0$.

This has, again, been taken from [22], and has a second harmonic content of only 16.5%. The results, given in Table 4.5 and

Time(ms)	Input	OP	INR	RES	TRIP
0.25	0.000	-0.039	0.000	0.000	0.002
2.75	0.000	-0.039	0.000	0.000	0.002
5.25	0.058	0.083	0.515	0.003	0.002
7.75	0.126	0.212	0.885	0.010	0.002
10.25	0.149	0.261	0.634	0.022	0.002
12.75	0.115	0.271	1.070	0.027	0.002
15.25	0.042	0.409	1.150	0.027	0.002
17.75	0.000	0.522	0.634	0.027	0.002
20.25	0.000	0.491	0.634	0.027	0.002
22.75	0.000	0.522	0.634	0.027	0.002
25.25	0.057	0.489	0.634	0.027	0.002
27.75	0.126	0.522	0.634	0.027	0.002
30.25	0.149	0.491	0.634	0.027	0.002
32.75	0.115	0.522	0.634	0.027	0.002
35.25	0.042	0.489	0.634	0.027	0.002
37.75	0.000	0.522	0.634	0.027	0.002
40.25	0.000	0.491	0.634	0.027	0.002
42.75	0.000	0.522	0.634	0.027	0.002
45.25	0.057	0.489	0.634	0.027	0.002
47.75	0.126	0.522	0.634	0.027	0.002
50.25	0.149	0.491	0.634	0.027	0.002

Table 4.4 Simulated results for relay performance during a 1-ϕ inrush current flow

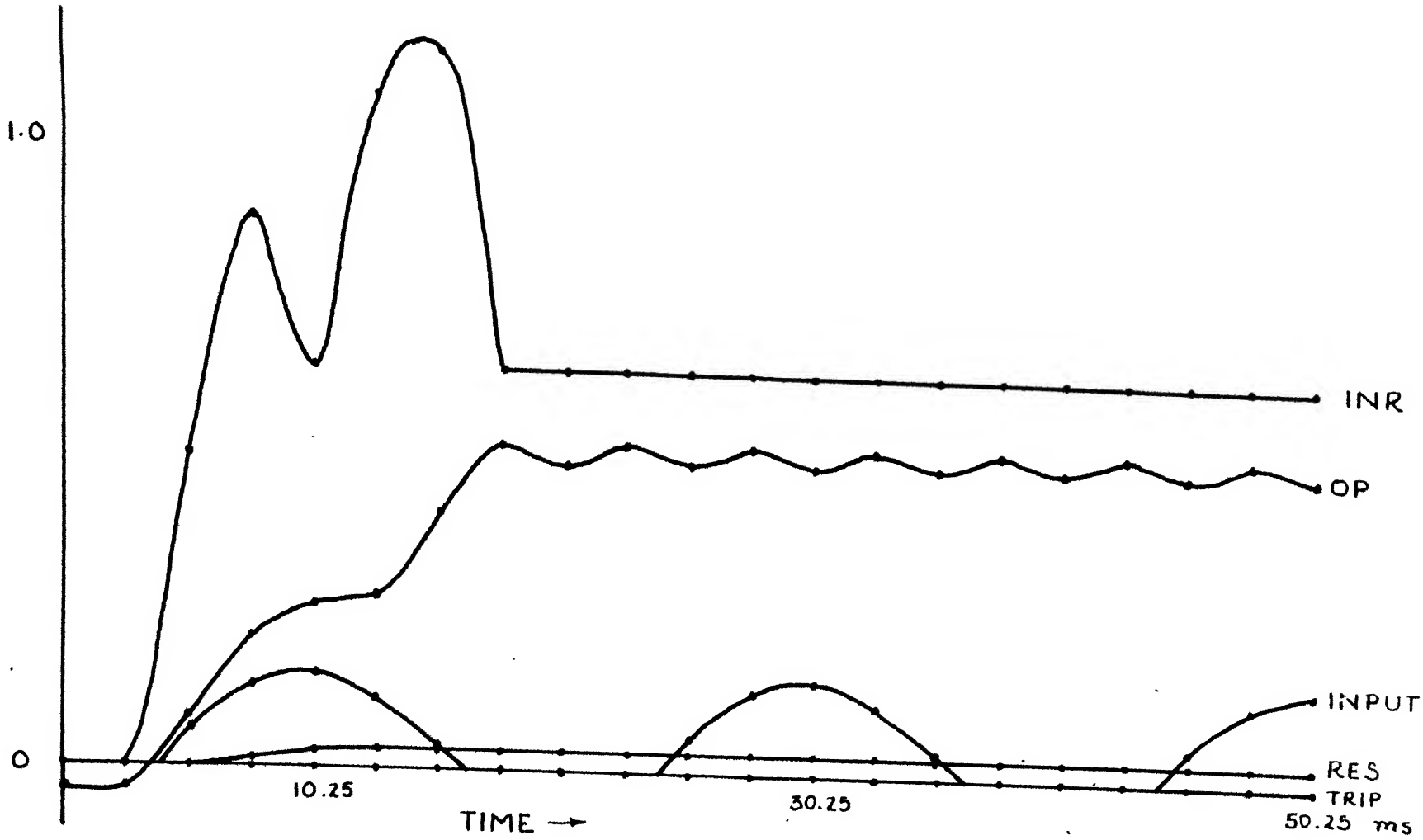

FIG. 4·6 : RELAY PERFORMANCE FOR 1-Φ INRUSH CURRENT

Fig. 4.7, again show that tripping is avoided by a comfortable margin.

Table 4.6 shows the results of some studies designed to test various new features of the proposed scheme. A brief look at the last two columns shows that the variable bias feature is working, exactly as envisaged. Another point to be noted is that the relay always overestimates the rms value of the mean through current, as asserted in Section 4.2.4.

In the first simulation, tripping occurs as expected. The next simulation is similar in nature, and was designed to test the variable bias factor provision. In the third simulation, the TAP input is set to -0.8. This reduces $\bar{I}_1$ by 10%, and tripping does not occur. Under the same conditions, a phase difference is introduced, in the fourth simulation, between $\bar{I}_1$ and $\bar{I}_2$, which again causes tripping.

The first three results of table 4.6 were verified on the hardware that has been developed.

4.6 Conclusion

We have found that all features described in the earlier part of this chapter work satisfactorily. The relay performance is expected to deteriorate sharply as the operating frequency

Table 4.5

Time (ms)	Input	OP	INR	RES	TRIP
0.25	0.000	-0.039	0.000	0.000	0.002
2.75	0.033	0.010	0.277	0.001	0.002
5.25	0.148	0.274	1.202	0.009	0.002
7.75	0.220	0.418	1.295	0.027	0.002
10.25	0.192	0.408	1.493	0.046	0.002
12.75	0.115	0.537	1.784	0.045	0.002
15.25	0.042	0.719	1.546	0.042	0.002
17.75	0.000	0.801	1.030	0.039	0.002
20.25	0.000	0.801	1.030	0.042	0.002
22.75	0.033	0.799	1.030	0.039	0.002
25.25	0.148	0.800	1.030	0.042	0.002
27.75	0.220	0.801	1.030	0.039	0.002
30.25	0.192	0.801	1.030	0.042	0.002
32.75	0.115	0.799	1.030	0.039	0.002
35.25	0.042	0.800	1.030	0.042	0.002
37.75	0.000	0.801	1.030	0.039	0.002
40.25	0.000	0.801	1.030	0.042	0.002
42.75	0.033	0.799	1.030	0.039	01002
45.25	0.148	0.800	1.030	0.042	0.002
47.75	0.220	0.801	1.030	0.039	0.002
50.25	0.192	0.801	1.030	0.042	0.002

Table 4.5 Simulated results for relay performance during a 3-ϕ inrush current flow

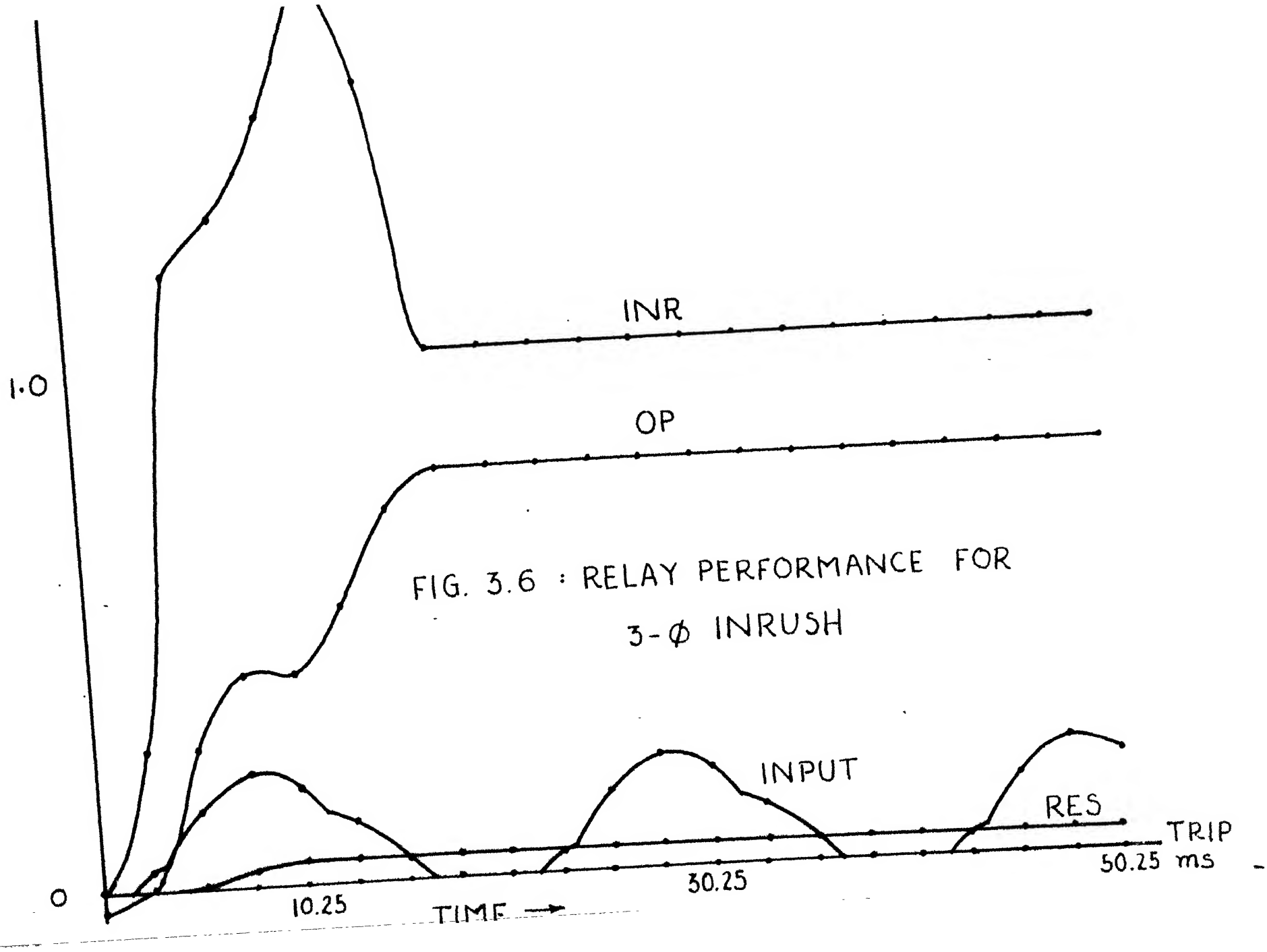

FIG. 3.6 : RELAY PERFORMANCE FOR 3-ϕ INRUSH

I_{1rms}	I_{2rms}	∅	TAP	AVG	RES	TRIP	RES/AVG	S=0.0625+AVG
0.1	0.2	0.0	0.0	0.162	0.036	0.877	0.223	0.224
0.2	0.3	0.0	0.0	0.272	0.090	0.877	0.332	0.334
0.3	0.2	0.0	-0.8	0.256	0.081	0.002	0.316	0.318
0.3	0.2	8.9	-0.8	0.226	0.064	0.877	0.285	0.288

Table 4.6 Steady state response of the proposed relaying scheme

∅ is the phase different between $\bar{I}_1$ and $\bar{I}_2$. AVG is the mean through current. RES = S * AVG.

All outputs have been taken after 20.25 ms of simulation (The entries marked with an asterisk are not relay outputs).

varies from 50 Hz, although this has not been verified experimentally.

The results obtained indicate that the relay can be expected to be highly reliable and fast in operation.

CHAPTER 5

CONCLUSION

A percentage differential relay for transformer protection using harmonic restraint to avoid tripping due to magnetizing inrush current has been designed, fabricated, and tested. The hardware realization uses the Intel 2920 Analog Signal Processor. Digital signal processing techniques have been used, giving more flexibility, reliability, and higher speed of operation.

The main objective of hardware simplification has been achieved to a very large extent. This will lead to ease in maintenance and repair. Identical units have been used for all the phases of a three-phase transformer, which would again help in maintenance. The protection of each phase is independent of the other phases.

Several unique features have been added to the conventional scheme of unit protection. These include provision for taking tap changing into account, and variable bias factor for greater sensitivity. A new method of approximating the rms value of harmonics from the corresponding sine and cosine wave amplitudes has been tried out successfully.

The relay requires very little power to operate, and would impose very low burden on the current transformers used for monitoring winding currents small changes in component values are hardly expected to cause any change in the performance of the relay (i.e., the relay is insensitive to component values). Simple hardware would lead to low cost also.

The tests and simulations performed reveal that the relay can be expected to perform satisfactorily in actual operation.

One of the major limitations of the proposed relay is its high sensitivity to frequency fluctuations. A careful look at the frequency response of Haar filters (Fig. 3.4) reveals that the attenuation of undesirable harmonics decreases sharply as the operating frequency changes from 50 Hz. As a result, the relay may not perform as envisaged if the operating frequency changes significantly.

Some provision to make the relay self checking could also be introduced.

Another drawback is the use of 8 sample Haar transforms for filtering. If the phenomenon of over voltage inrush (caused by switching) is also to be taken into account, we must use 16 sample Haar transforms. This might be possible using some more recent integrated circuits like Intel 8748 (single chip microcomputer) and some others. This possibility needs to be explored.

References

[1] Cordray, R.E., Percentage Differential Transformer Protection, Electrical Engineering, vol. 50, May 1931, pp 361-363.

[2] Kennedy, Hayward, Harmonic Restrained Relays for Xmer Protection, Trans. AIEE, vol. 57, 1938, p 262.

[3] Hayward, C.D., Harmonic Current Restrained Relays for Xmer Differential Protection, AIEE Trans., vol. 60, 1941, pp 377-382.

[4] Bertula, G., Enhanced Xmer Protection through Inrush-proof Ratio Differential Relays, Brown Boveri Review, vol. 32, 1945, p 129.

[5] Wellings, Mathews, Instantaneous Magnetic Balance Protection for Power Xmers, B.T.H. Activities, vol. 191, 1946, p 30.

[6] AIEE Relay Sub-committee, Relay Protection of Power Xmers, Trans. AIEE, vol. 66, 1947, pp 911-916.

[7] Leybern, Lackey, Protection of Electric Power Systems, a Critical Review of Present Practice and Recent Progress, proc. IEE, vol. 98, Part 2, Feb 1951, pp 47-66.

[8] Klingshirn, Moore, Wentz, Detection of faults in power systems, Trans. AIEE, vol. 76, 1957, Part 3.

[9] Sharp, R.L. and Glassburn, W.E., A Xmer Differential Relay with Second Harmonic Restraint, Trans. AIEE, vol. 77, Part 3, pp 913-918, Dec. 1958.

[10] Rockfeller, G.D., Fault Protection with a Digital Computer, IEEE Trans. PAS-88, pp 438-464, April 1969.

[11] Sykes, J.A. and Morrison, I.F., 'A Proposed Method for Harmonic Restraint Differential Protection for Power Xmers', IEEE Trans. PAS-91, pp 1260-1272, 1972.

[12] Malik, O.P., Dash, P.K. and Hope, G.S., 'Digital Protection of Power Xmer', Proc. IEEE PES Winter Meeting, New York, USA, Jan 1976, Paper A76 191-7.

[13] Larson, R.R., Flechsig, A.J. and Schweitzer, E.O., 'The Design and Test of a Digital Relay for Xmer Protection', IEEE Trans. PAS 98, pp 795-804, 1979.

[14] Degens, A.J., 'μP Implemented Digital Filters for Inrush Current Detection', Int. J. Elect. Power and Energy Syst., vol. 4, No.3, pp 196-205, July 1982.

[15] Thorp, J.S. and Phadke, A.G., 'A μP Based 3-Ø Xmer Differential Relay', IEEE Trans. PAS-101, pp 426-432, Feb. 1982.

[16] Rahman, M.A. and Dash, P.K., 'Fast Algorithm for Digital Protection of Power Transformers', Proc. IEE, vol. 129, Part C, Mar 1982, pp 79-85.

[17] Fakruddin, D.B., Parthasarthy, K., Jenkins, L. and Hogg, B.W., 'Application of Haar functions for transmission line and transformer differential protection', El. Power and Energy Systems, vol. 6, No.3, July 1984, pp 169-180.

[18] A.R. Warrington, 'Protective Relays - their Theory and Practice', Chapman and Hall Ltd., 1971 (Reprint), 2nd Edition.

[19] Blume, L.F., Camilli, G., Farnham, S.B., and Peterson,H.A., 'Transformer Magnetizing Inrush Currents and Effect on System Operation', AIEE Trans., 1944.

[20] 'Report on Magnetizing Inrush Current and its Effect on Relaying and Air Switch Operation', AIEE Committee, Trans. AIEE, vol. 70, Part II, 1951.

[21] Specht, T.R., 'Transformer Magnetizing Inrush Current', AIEE Trans., vol. 70, Part I, 1951, pp 323-328.

[22] Sonnemann, W.K., Wagner, C.C., Rockfeller, G.D., 'Magnetizing Inrush Phenomenon in Transformer Banks', Power Apparatus and Systems, Oct. 1958, pp 884-892.

[23] Specht, T.R., 'Transformer Inrush and Rectifier Transient Currents', IEEE Trans. Power Apparatus and Systems, vol. 88, April, 1969, pp 269-276.

[24] Schweitzer, E.O., Larson, R.R. and Flechsig, A.J., 'An efficient inrush current algorithm for digital computer relaying, protection of transformers', Proc. IEEE PES Summer Meeting Mexico (July 1977).

[25] Electronic Filter Design Handbook, Arthur B. Williams, McGraw-Hill, 1981.

[26] Handbook of filter synthesis, Anatol I, Zverev, John Wiley and Sons Inc., 1967.

[27] Picture Processing and Digital Filtering, 2nd edition, Edited by T.S. Huang, Springer-Verlag Berlin Heidelberg New York, p 47.

[28] Haar, A., 'Zur theorie der orthogonalen Functionensysteme' Math. Annal. 69, 1910, pp 331-71.

[29] Alexits, O., 'Convergence Problems of Orthogonal Series', Pergamon Press, New York and London, 1961.

[30] Shore, J.E., 'On the application of Haar functions', IEEE Trans. Communications, COM 21, 3, 1973.

[31] 2920 Analog Signal Processor Design Handbook, Intel Corporation, August 1980.

[32] 2920 Simulator User's Guide, Intel Corporation.